Lamine Boumaiza[1], Julien Walter[2,3], Romain Chesnaux[2,3], Frédéric Huneau[4,5], Émilie Garel[4,5], Mélanie Erostate[4,6], Karen H. Johannesson[7], Yuliya Vystavna[8], Nabil Bougherira[9], Geneviève Bordeleau[10], Randy L. Stotler[1], Mónica Blarasin[11], Mélida Gutiérrez[12], Kay Knöller[13], Christine Stumpp[14]

[1] University of Waterloo, Department of Earth and Environmental Sciences, Waterloo (Ontario), N2T 0A4, Canada

[2] Université du Québec à Chicoutimi, Département des Sciences Appliquées, Saguenay (Québec), G7H 2B1, Canada

[3] Centre d'études sur les ressources minérales, Groupe de recherche Risque Ressource Eau, Saguenay (Québec), G7H 2B1, Canada

[4] Université de Corse Pascal Paoli, Département d'Hydrogéologie, Campus Grimaldi, Corte, 20250, France

[5] CNRS, UMR 6134 SPE, Corte, 20250, France

[6] Institution Adour, Service gestion intégrée - Mission nappes profondes, Mont-de-Marsan, 40000, France

[7] University of Massachusetts Boston, School for the Environment, Boston, Massachusetts, 02125, USA

[8] International Atomic Energy Agency, Isotope Hydrology Section, Vienna, 1400, Austria

[9] Université Badji Mokhtar, Département de Géologie, Campus de Sidi-Amar, Annaba 23005, Algeria

[10] Institut national de la recherche scientifique, Centre Eau Terre Environnement, Québec (Québec), G1K 9A9, Canada

[11] Universidad Nacional de Río Cuarto, Departamento de Geología, Río Cuarto, Córdoba, X5804BYA, Argentina

[12] Missouri State University, Department of Geography, Geology and Planning, Springfield, Missouri, 65897, USA

[13] Helmholtz Centre for Environmental Research, Department of Catchment Hydrology, Halle (Saale), 06120, Germany

[14] University of Natural Resources and Life Sciences, Institute of Soil Physics and Rural Water Management, Vienna, 1190, Austria

Corresponding author: E-mail address: lamine.boumaiza@uwaterloo.ca (L. Boumaiza)

Multi-tracer approach to understand nitrate contamination and groundwater-surface water interactions in the Mediterranean coastal area of Guerbes-Senhadja, Algeria

Abstract

Implementing sustainable groundwater resources management in coastal areas is challenging due to the negative impacts of anthropogenic stressors and various interactions between groundwater and surface water. This study focuses on nitrate contamination and transport via groundwater-surface water exchange in a Mediterranean coastal area (Guerbes-Senhadja region, Algeria) that is heavily affected by anthropogenic activities. A multi-tracer approach, integrating hydrogeochemical and isotopic tracers ($\delta^{2}H_{H2O}$, $\delta^{18}O_{H2O}$, ^{3}H, $\delta^{15}N_{NO3}$ and $\delta^{18}O_{NO3}$), is combined with a Bayesian isotope mixing model (MixSIAR) to (i) elucidate the nitrate sources and their apportionments in water systems, and (ii) describe potential interactions between groundwater and surface water. Results from nitrate isotopic composition and the MixSIAR model show that nitrate concentrations mainly originate from sewage and manure sources. Nitrate derived from the sewage is attributed to urban and rural wastewater discharge, whereas nitrate derived from the manure is related to animal manure used to fertilise agricultural areas. High apportionments of nitrate-based atmospheric precipitation are identified in groundwater and surface water; a finding that is specific to this study. The multi-origin stresses combined with evidence of interactions between surface water and groundwater contribute to negatively impacting large parts of the study coastal area. The outcomes of this study are expected to contribute to sustainable management of coastal ecosystems by drawing more attention towards groundwater use and protection. Furthermore, this study may improve scientists' ability to predict the behavior of anthropogenically impacted coastal ecosystems and help decision-makers elsewhere to prepare suitable environmental strategies for other coastal ecosystems currently undergoing an early stage of groundwater resources deterioration.

Keywords

Nitrate, Isotope tracers, Aquifer, Groundwater, Surface water, MixSIAR

1 Introduction

Coastal areas commonly contain aquatic ecosystems that contribute to rich biodiversity as they provide habitat and food resources for wildlife and estuarine, marine, and terrestrial fauna (Camacho-Valdez et al., 2013; Clara et al., 2018; Newton et al., 2018). These ecosystems include a variety of surface water systems (SWSs; e.g., swamps, inlets, marshes, and lagoons) that locally control the hydrological cycle by contributing to surface water retention (Rao et al., 2015; Velasco et al., 2018). However, large amounts of the surface water stored in coastal ecosystems can be supplied by groundwater, which is why many are commonly classified as groundwater-dependent ecosystems (Erostate et al., 2020; Menció et al., 2017; Stumpp et al., 2014). The human population may depend directly on these coastal ecosystems for numerous activities including tourism, agriculture, fisheries, and aquaculture exploitation (Clara et al., 2018; Lyra et al., 2021; Willaert, 2014). Therefore, these ecosystems have direct economic value, in addition to their intrinsic somewhat less easily quantified value of the ecosystem service functions that they provide. Many of these ecosystems are protected by legal regulations, through national/international conventions (e.g., Barcelona Convention for the Protection of the Mediterranean Sea) to sustainably manage human activities at all scales. However, the uncontrolled human exploitation of coastal areas, combined with other harmful practices, such as industrial and domestic discharges, result in groundwater resource deterioration that affects the ecosystem functions (Barhoumi et al., 2014; David et al., 2019; Pittalis et al., 2018). Increased nutrient inputs, enhanced by urban, agricultural, or industrial discharges affects groundwater quality and leads to anthropogenic eutrophication of SWSs. Such practices disturb the SWSs deteriorating and damaging the ecosystem functions, and consequently,

reducing their intrinsic and economic benefits (Erostate et al., 2022; García and Muñoz-Vera, 2015).

The scientific community must collectively address such interdisciplinary problem. Hydrogeologists conceptualized surface water and groundwater flux as determinant factors that control the ecosystems (Erostate et al., 2020). From this conceptualization, environmental legislation has been enacted in many locations around the world that requires an integrated approach (e.g., USGS National Water Quality Assessment Program (Leahy et al., 1990)), in which both surface water and groundwater are considered together when developing ecosystem management strategies. However, implementing efficient and sustainable groundwater resources management for coastal areas is challenging due to the impact of multi-anthropogenic stressors combined with the various interactions between groundwater and surface water (Clara et al., 2018; Erostate et al., 2022, 2019). Some known examples of Mediterranean coastal systems, experiencing intensive agricultural activities, have caused serious deterioration of local groundwater resources (Boumaiza et al., 2022; Lyra et al., 2021; Rachid et al., 2021). To establish efficient and sustainable combined management of groundwater and surface water resources in coastal ecosystems, field-based case studies are needed. To this end, impacted coastal areas provide an opportunity to research the challenges faced by many ecosystems around the world, especially in regions with uncontrolled land use development. Coastal ecosystems occupy approximately 13% of the world's coastlines, with a contribution estimated to 18% of the Africa coastline (Barnes, 1980; Kjerfve, 1994). In North Africa, coastal ecosystems are widely distributed from the Atlantic Ocean to the southeastern coastline of the Mediterranean Sea through Morocco, Algeria, Tunisia, Libya, and Egypt (El Mahrad et al., 2020). The present study

provides results from a field-based research program, which was guided through an Algerian coastal complex area where ecosystems are heavily affected by multiple anthropogenic activities, to construct a comprehensive understanding on how these coastal ecosystems are affected by anthropogenic stresses.

Algeria contains several coastal areas of international importance including the selected coastal Mediterranean area of Guerbes-Senhadja, a 2011-recognized Ramsar site emphasizing the international relevance of the selected study area. The Guerbes-Senhadja region contains several SWSs distributed over an area of complex geomorphology featuring a multitude of depressions and valleys, sandy dunes, rivers, estuaries, beaches, and sea cliffs. It is a significantly important site for tourism, having high agricultural potential, and rich biodiversity sheltering many plant and animal species (Babouri et al., 2020; Bouchaala et al., 2017; Samraoui and De Belair, 1997). However, this site of important ecological and socioeconomic values is disturbed by several anthropogenic stressors including land-clearing, fires, overgrazing, sand pit exploitation, uncontrolled growing urbanization, unmanaged agricultural expansion combined with unsafe agricultural practices, and excessive extraction of groundwater and surface water for irrigation and domestic purposes (Toubal et al., 2014). All these anthropogenic stressors seriously impact the study area, where several degrading signs have been observed such as the erosion of river banks and littoral, sandy dunes destabilization, silting up of fertile lands, and water quality deterioration (Hedjal et al., 2019; Toubal et al., 2014). Despite the increased uncontrolled land use, the total surface of the study area is still made up approximately of 80% of agricultural lands, which are dominated by production of legumes in open agricultural fields. The direct uncontrolled application of nitrogen-based fertilizers

to agricultural lands of the study area suggests that the identified harmful nitrate (NO_3) concentrations in groundwater (NO_3 up to 97 mg/l) can be attributed to contributions from unsafe agricultural practices (Hadj-Said, 2007). However, this conclusion has yet to be verified by advanced source tracking tools such as stable isotope analyses or statistical-based interpretation. Rivers crossing the Guerbes-Senhadja region receive urban and industrial wastewater discharges without pre-treatment (Bouleknafet and Derradji, 2017; Toubal et al., 2014). This suggests that high NO_3 concentrations in groundwater could also be attributed to contribution from potential wastewater influx, as wastewater and associated contaminants from urban/industrial discharges could infiltrate into the aquifer or originate from interactions between groundwater and surface water (McCance et al., 2018; Vystavna et al., 2019).

This paper presents a preliminary study aiming (i) to distinguish the main sources of groundwater quality deterioration within the coastal area of Guerbes-Senhadja, with focus on anthropogenic NO_3 contamination, and (ii) to describe potential groundwater-surface water interactions, by investigating the potential relationship between surface water and groundwater at the investigated sampling site, that contribute to transporting impacted water over the coastal aquifer. A multi-tracer approach is used that integrates major chemical elements, stable water isotopes (δ^2H_{H2O} and $\delta^{18}O_{H2O}$), stable nitrate isotopes ($\delta^{15}N_{NO3}$ and $\delta^{18}O_{NO3}$), the radioactive isotope tritium (^3H), and a Bayesian isotope mixing model (MixSIAR). Furthermore, we argue that our approach may improve scientists' ability to predict the hydrogeological behavior of anthropized complex coastal areas, and will help groundwater managers from other regions to prepare suitable environmental plans for coastal ecosystems undergoing an early stage of groundwater resources deterioration.

2 Setting of study area

2.1 *Geographic location and hydrologic features*

The study area is the Guerbes-Senhadja wetland located 25 km east of the City of Skikda in northeastern Algeria (Figure 1). The study area constitutes a large coastal valley separating the Felfela-Senhadja Mountains, featuring an altitude varying from 330 m above sea level (a.s.l.) (Djebel Safia) to 541 m a.s.l. (Djebel El-Foul), at the west and the Chetaïbi Mountains, presenting an altitude reaching up to 510 m a.s.l., at east. Further south, the study area connects to a large flat valley constituting the Plain of Ben-Azouz, whereas the northern boundary is the Mediterranean Sea over a shoreline of roughly 15 km. The Guerbes-Senhadja area is mainly crossed by the "El-Kebir River" —flowing south to north— from which two other rivers are tributary, i.e., the "Maboune River" in the southwest and the "Magroune River" in southeast of the study area (Figure 1). The study site covers approximately 200 km^2, on which there are some urban villages including Ben-Azouz, Guerbes, and Zaouia villages, next to other small rural communities such as Ouled-Malek, Gaïd-Lakhdar, Ain-Nechema, and Dem El-Begrat. The Guerbes-Senhadja region is an alluvial system wherein half of the study area features slopes varying from 3 to 13% (Boussehaba, 2010). This landscape physiography provides a multitude of depressions and valleys forming several SWSs (locally called "Merdja" or "Garâa") featuring shallow water depths ranging from 0.5 to 3 m below ground surface (Bouchaala et al., 2017). Several other small SWSs (<0.01 km^2) exist within the study area; most of them are the result of artificial digging by local farmers for providing surface water used for irrigating the agricultural lands.

The Guerbes-Senhadja region is characterised by Mediterranean climate conditions featuring two main distinct periods: (i) a wet period, occurring from October to April, with monthly average temperature of +14°C; and (ii) a dry period, occurring from May to September, with monthly average temperature of +26°C (Hedjal, 2019). The study area captures an average annual rainfall precipitation amount of about 687 mm including 594 mm over the wet period (October-April), whereas 93 mm are received during the dry period (May-September). The mean annual actual evapotranspiration was estimated at 456 mm, including 263 mm for the wet period and 193 mm corresponding to the dry period (Hedjal, 2019). During the wet period, the excess of precipitation over evapotranspiration leads to considerable aquifer recharge. Conversely, the dry period features an evapotranspiration rate exceeding precipitation that accordingly leads to enhanced evaporation from both SWSs and groundwater tables.

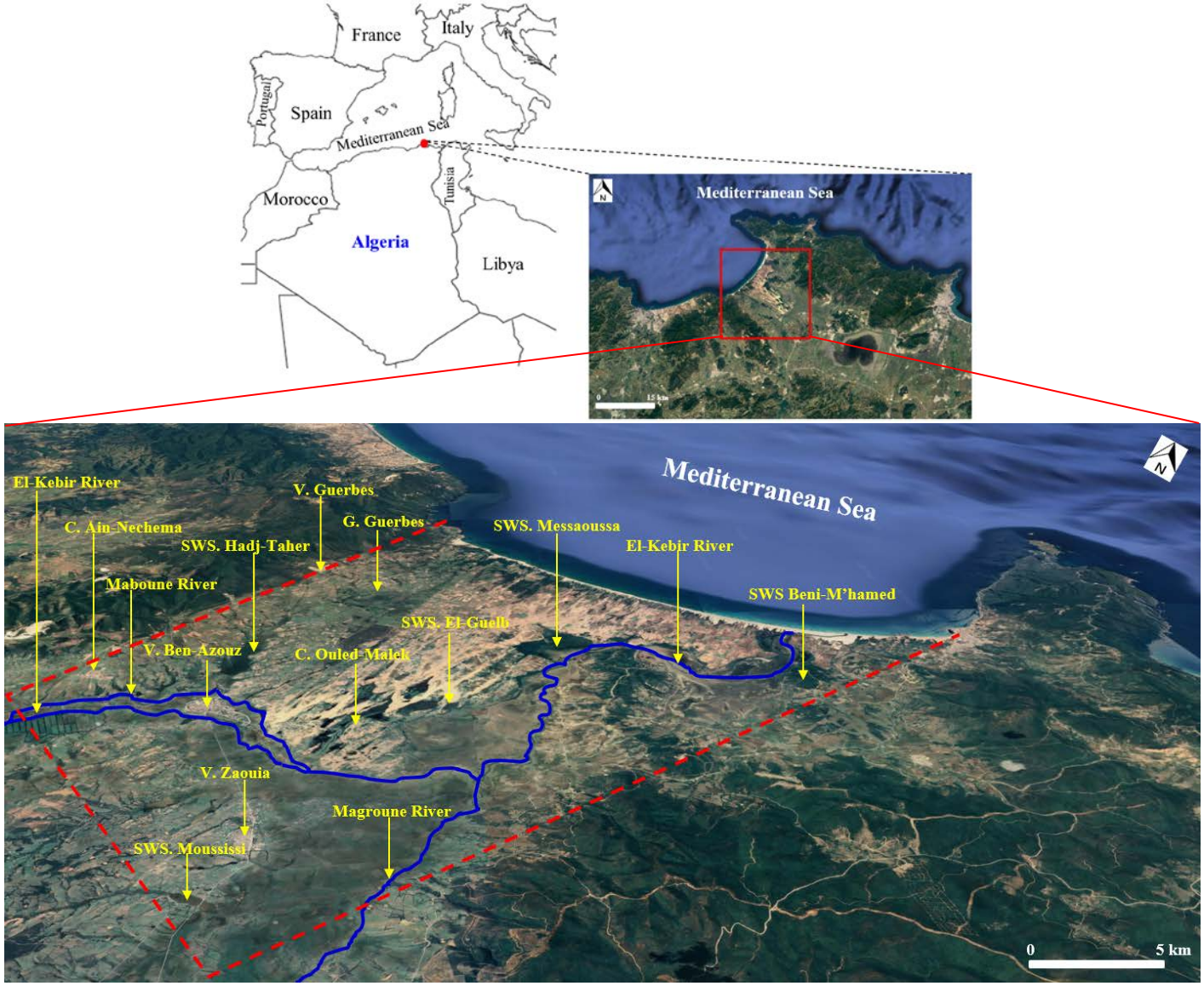

Figure 1. Geographic location of study area with a perspective overview. Here, is indicated the location of the main large villages (e.g., V. Ben-Azouz), some small rural communities (e.g., C. Ain-Nechema), some SWSs (e.g., SWS. Hadj-Taher), and the main rivers crossing the study area (e.g., El-Kebir River). In dashed red is the approximate limit of the study area.

2.1 *Geology, geomorphology and hydrogeological background*

The Guerbes-Senhadja region belongs to the Algerian coastal magmatic chain, which is considered as part of the internal zones of the North Africa Alpine chain —originating from tectonic activity in the occidental Mediterranean basin— associated with the collision of the African and European tectonic plates during the Oligo-Miocene period (Auzende et al., 1975; Cohen, 1980; Letouzey and Trémolières, 1980; Vila, 1980). The study area corresponds to a Neogene subsiding graben limited by two major fault systems, which caused large, kilometric-scale landslides during the last Alpine phase of the Miocene. This tectonic event placed the African plate and the European plate, represented respectively by the Edough Complex to the east and the Felfela Basement to the west, at the same latitude. The geological context of these formations includes metamorphosed granitoid rocks (Figure 2), which are partly covered by a system of folded sedimentary rocks resulting from tectonic activity. These folded sedimentary rocks are composed of Cretaceous marls/sandstones (Cretaceous flysch) and Oligo-Miocene sandstones (Numidian flysch) (Joleaud, 1936; Llavsky and Snopkova, 1987). Edough Metamorphic Rock Complex was isolated from the Felfela and stood with sufficient relief that it was an island when the sea invaded the region during the Pliocene (Hilly, 1962). However, sedimentary inputs from the mainland progressively filled of the shallow basins located at the southern and eastern limits of the Edough Metamorphic Rock Complex; the later subsequently became linked to the African Continent since the early Quaternary. Further, the Edough Metamorphic Rock Complex-shoreline has continued to evolve from south to north, leading to the deposition of large accumulations of Quaternary deposits within the subsiding graben of Guerbes-Senhadja (Figure 2).

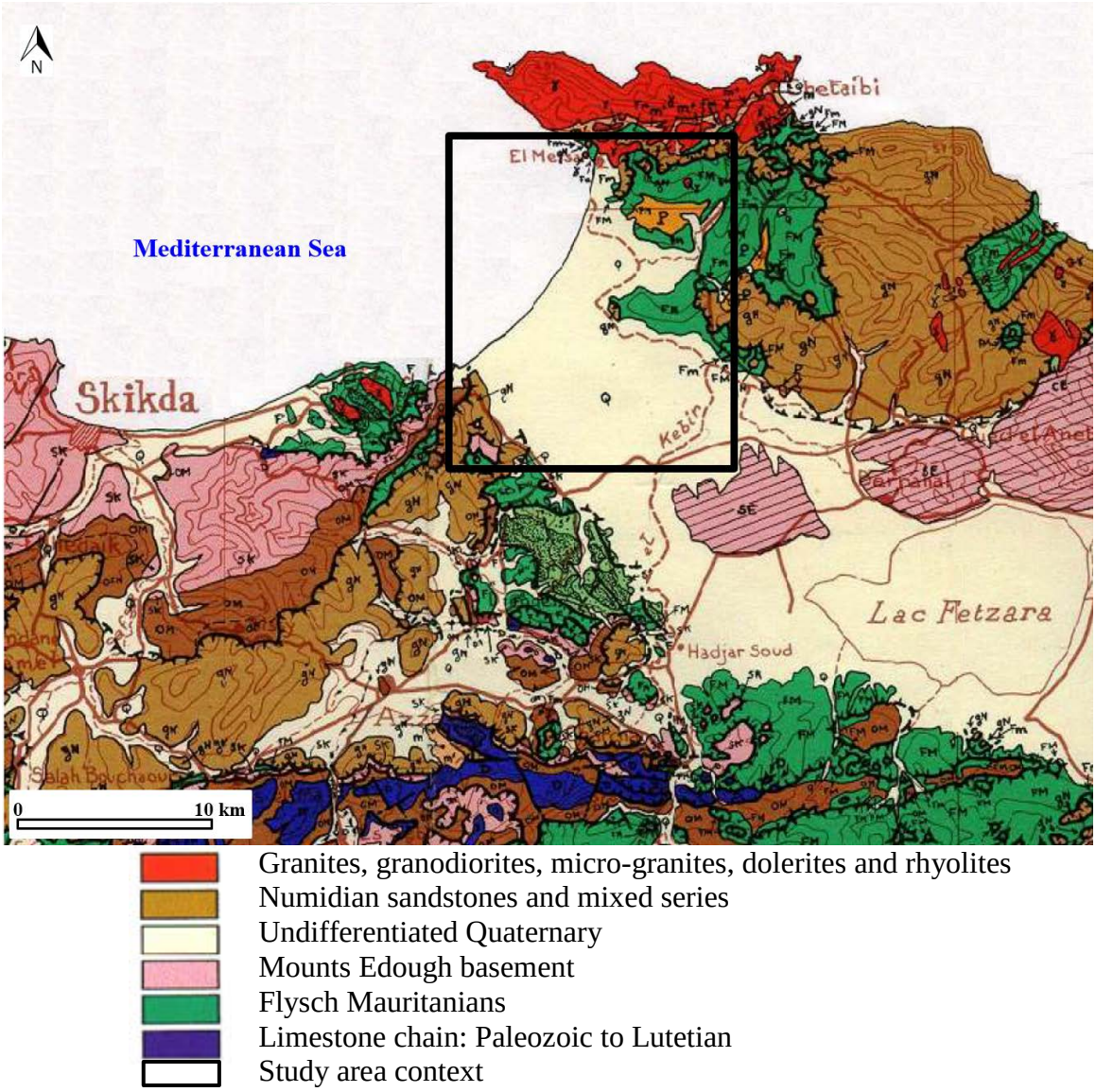

Figure 2. Main geological setting of the study area (Vila, 1980).

During the late Quaternary period, predominant north-western/south-eastern winds formed an 8,000-ha region of sandy dunes over the Guerbes-Senhadja region. The effect of the winds decreased inland from the sea, such that these sandy dune deposits are common and relatively thick along the coast, and are much reduced inland. These sandy dune deposits are also rich in impermeable clay lenses that probably reflect avulsions of the El-Kebir River on its north-eastern side, whereas the obstruction of the river bed

combined with the gentle slope of terrain fostered the extension of the alluvial plain, thereby creating a series of depressions during the evolution process (Samraoui and De Belair, 1997). Together these events can explain the variable slopes within the study region that again range from 3 to 13% (Boussehaba, 2010; Hedjal et al., 2018). The low surface water drainage over the study area combined with high groundwater discharge from the sandy dune deposits promote the accumulation of surface water that has resulted in the formation of several SWSs (Samraoui and De Belair, 1997; Toubal et al., 2014). The subsiding graben of the Guerbes-Senhadja region is filled by Plio-Quaternary granular, lithogenic material corresponding to multiple origins, including eolian and fluvio-lacustrine deposits, that explain the diversity in lithofacies. Regarding the information from boreholes drilled in the study area, the Guerbes-Senhadja region contains an upper unconfined aquifer —varying from 50 to 140 m in thickness— mainly composed of sandy material overlying clay deposits with a mean thickness of 5 m (Hedjal, 2019) that constitutes the top of the deeper confined aquifer. The latter has a thickness varying from 12 to 50 m, and is composed of polygenic materials, gravels, and pebbles presumably resting on substratum formed by alternating sandstone and marl (Bouleknafet and Derradji, 2017; Toubal et al., 2014). The upper and deeper aquifers are directly connected in some locations of the study area where the clayey aquitard separating them is practically nonexistent (Hedjal, 2019). Chemical analyses of groundwater samples collected from the upper aquifer in 2013 (Bouleknafet and Derradji, 2017) and 2016 (Hedjal et al., 2018) revealed sodium-chloride and magnesium-chloride water types.

3 Material and methods

3.1 Sampling and laboratory analyses

3.1.1 Sampling network and protocol

The present study included both a surface water and groundwater sampling program, which was performed on November 20-22, 2021. Here, 10 groundwater samples were collected over the study area, 14 surface water samples were collected from SWSs and the main rivers crossing the study area (Figure 3), one sample was collected from the Mediterranean Sea, and one from rainfall. It should be mentioned that the choice of the sampling sites is essentially based on their accessibility. Groundwater samples were collected from shallow private wells that were dug by the owners in the unconsolidated sediments; these wells feature a diameter varying overall from 2 to 3 m and groundwater depth of 3−6 m below ground surface. Surface water samples were collected as grab samples directly from the streams. During water sampling, the physico-chemical parameters (temperature, pH, electrical conductivity (EC), total dissolved solid (TDS)) —both for groundwater and surface water— were measured in-situ using a calibrated multiparameter probe (HI-9829, Hanna Instruments©). The water collected for major anion and cation chemical analyses was filtered in-situ through 0.45-μm nitrocellulose membrane filters attached to 100-mL luer-lock syringe samplers and subsequently pushed through the filters into two separate 40-mL amber glass bottles. The bottles for cation analysis were acidified to pH <2 by adding 2−3 drops of ultrapure nitric acid (HNO_3) with the aim to prevent major cations precipitation or adsorption during storage. Water samples for δ^2H_{H2O} and $\delta^{18}O_{H2O}$ analyses were collected in 40-mL amber glass bottles; whereas filtered water for $\delta^{15}N_{NO3}$ and $\delta^{18}O_{NO3}$ analyses were collected in 50-mL polyethylene bottles. The water for ^3H analysis

was collected in 500-mL polyethylene bottles. All sample bottles were completely filled with water without head-space and bottles were equipped with caps containing Teflon septa parafilm to prevent evaporation. During fieldwork, the water samples were temporarily stored in a portable cooler, before being transferred to a refrigerator for storage at +4°C, and further transported to the laboratories. The samples collected for stable nitrate isotope analyses were stored frozen, to avoid variations caused by biological processes, until the isotopic analyses were performed in the laboratory. All the water samples collected in this study (26 samples) were analyzed for the major elements and $\delta^{2}H_{H2O}$ and $\delta^{18}O_{H2O}$. Seventeen samples were analyzed for $\delta^{15}N_{NO3}$ and $\delta^{18}O_{NO3}$, whereas seven samples were analyzed for ^{3}H.

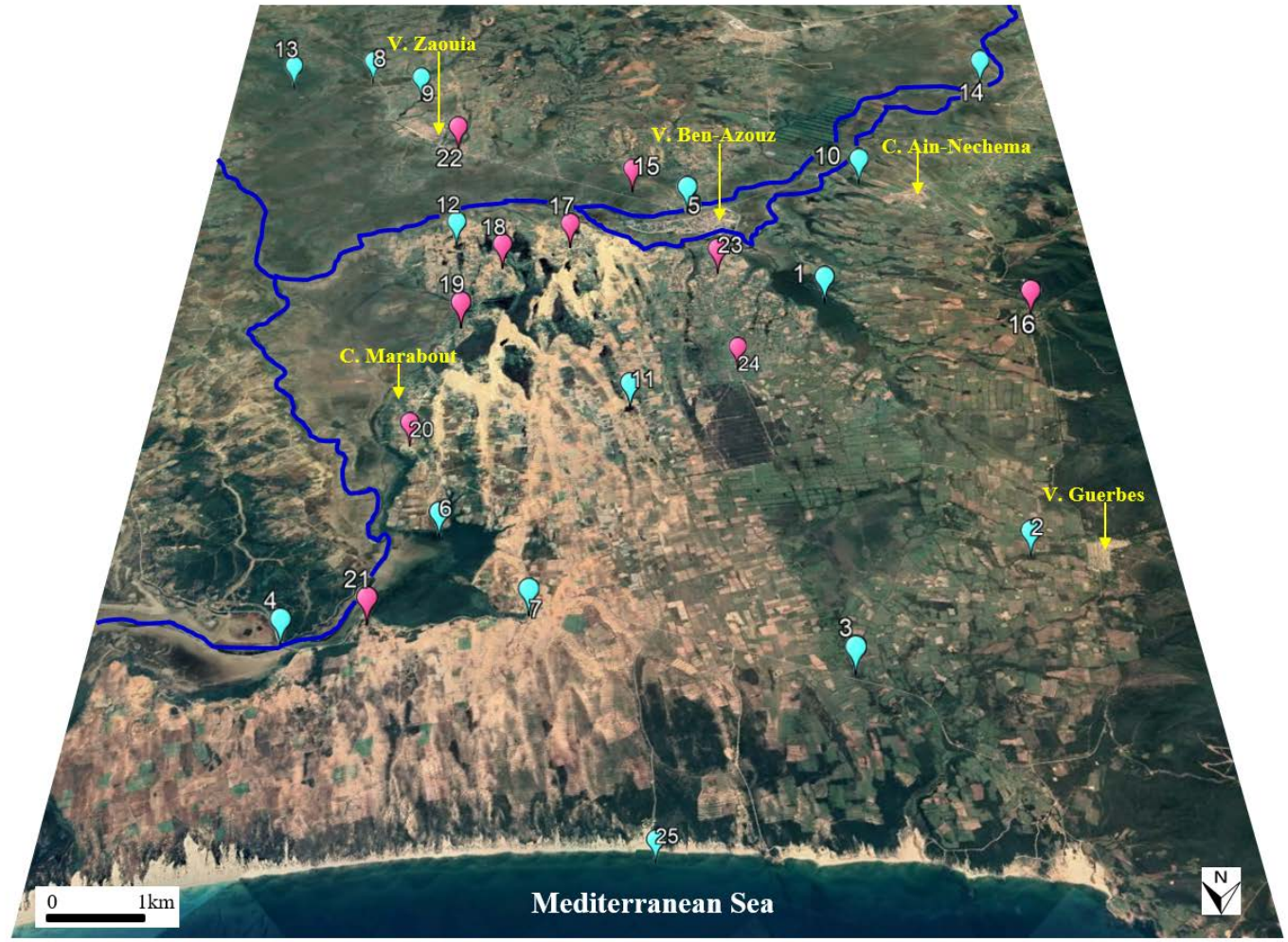

Groundwater sample Surface water sample

Figure 3. Location of surface water and groundwater samples collected over the study area. The numbered surface water samples are (#1) Hadj-Taher SWS, (#2) Gerbes 1 SWS, (#3) Gerbes 2 SWS, (#4) El-Kebir River downstream, (#5) El-Kebir River at Ben-Azouz, (#6) Messoussa SWS, (#7) Tributary Messoussa SWS, (#8) Moussisi SWS, (#9) Zaouia SWS, (#10) Ain-Nechema SWS, (#11) Gaïd-Lakhdar SWS, (#12) El-Guelb SWS, (#13) Magroune SWS, and (#14) El-Kebir River upstream.

3.1.2 Chemical and isotope tracer analyses

The chemical analysis was carried out in several laboratories. The major chemical elements (HCO_3^-, NO_3^-, Cl^-, K^+, Mg^{2+}, NH_4^+, Na^+, Ca^{2+} and SO_4^{2-}) were analyzed at the Laboratory of the Hydrogeology Department of the University of Corsica (France). The major elements concentrations were measured using a Dionex ICS 1100 chromatograph (Thermo Fischer Scientific, Waltham, USA), except HCO_3 concentrations that were determined by volumetric titration to pH 4.5 using a digital titrator HACH (Hach Company, Loveland, CO, U.S.A). The results of major elements were validated by testing the ionic balance, for which a absolute value of 5% was considered acceptable (Appelo and Postma, 2005; Hounslow, 1995). Tritium was analyzed at the Wessling Laboratory at Budapest (Hungary). Water samples for ^3H were degassed and stored in dedicated glass bulbs for the accumulation of the tritium decay product. After a reconditioning period of one month, ^3H content was analyzed by electrolytic enrichment followed by liquid scintillation counting spectrometry (Kaufman and Libby, 1954; Thatcher et al., 1977). The obtained ^3H activities were corrected for radioactive decay back to the time of the precipitation event, and ^3H activities are expressed in tritium units (TU) with a precision of ±0.5 TU (1 TU equals a radioactivity concentration of 0.118 Bq/L). The analyses of stable water isotopes (δ^2H_{H2O} and $\delta^{18}O_{H2O}$) were performed at the Laboratory of the Institute of Soil Physics and Rural Water Management in Vienna (Austria). These water isotopic compositions were determined using a laser-based isotope analyzer (Picarro L2130-*i*) according to the analytical scheme recommended by the International Atomic Energy Agency (IAEA) (Penna et al., 2010). Nitrogen and oxygen isotopes of nitrate ($\delta^{15}N_{NO3}$ and $\delta^{18}O_{NO3}$) were analyzed at the Helmholtz Center for Environmental Research in Halle/Saale (Germany),

using the denitrifier method with bacteria strains of *Pseudomonas chlororaphis* (ATCC #13985 equal to DSM-6698) according to the protocols recommended by Casciotti et al. (2002) and Sigman et al. (2001). Here, the $\delta^{15}N_{NO3}$ and $\delta^{18}O_{NO3}$ isotopic composition produced from NO_3 was measured by gas isotope ratio mass spectrometry using a DELTA-V Plus mass spectrometer and a GasBench II from Thermo Scientific. The isotope values (expressed in δ‰) were calculated using Equation 1, where R_{sample} and $R_{standard}$ are the sample's and the standard's ratios of the heavier to the lighter isotope, i.e., $^{2}H/^{1}H$, $^{15}N/^{14}N$, or $^{18}O/^{16}O$.

$$\delta\ (‰) = \frac{R_{sample} - R_{standard}}{R_{standard}} \quad (1)$$

The $\delta^{2}H_{H2O}$, $\delta^{18}O_{H2O}$ and $\delta^{18}O_{NO3}$ values are reported relative to the Vienna Standard Mean Ocean Water (VSMOW), whereas the $\delta^{15}N_{NO3}$ values are reported relative to the nitrogen (N_2) in atmospheric air (AIR). The precision of the analytical instrument was generally better than ±0.5‰ for $\delta^{2}H_{H2O}$ and ±0.1‰ for $\delta^{18}O_{H2O}$; whereas the reproducibility for the $\delta^{15}N_{NO3}$ and the $\delta^{18}O_{NO3}$ measurements were ±0.6‰ and ±0.4‰, respectively.

3.2 Identifying nitrate sources and estimating their apportionments

Kendall's diagram (Kendall, 1998), combining $\delta^{15}N_{NO3}$ to $\delta^{18}O_{NO3}$ isotopic compositions with specific zones corresponding to sources of NO_3, was used in the present study to identify the potential sources of NO_3. These sources include NO_3-based atmospheric precipitation (AP), NO_3-based fertilizers (NOF), NH_4-fertilizers (NHF), soil organic nitrogen (SON), sewage and manure (S&M), and NO_3-based desert deposits (DD). Furthermore, a Bayesian stable isotope mixing model (MixSIAR model) (Stock et al., 2018) was used to estimate the contributions of the different NO_3 sources to each groundwater and surface water sample. Numerous studies have assessed the usefulness of

the MixSIAR model in apportioning the potential sources of NO_3 in water systems (e.g., Boumaiza et al., 2022; Cao et al., 2021; He et al., 2022; Li et al., 2022; Torres-Martínez et al., 2021). The MixSIAR model requires the values of $\delta^{15}N_{NO3}$ and $\delta^{18}O_{NO3}$ measured in water samples and the different end-member isotopic values of the sources of NO_3. In this study, the end-member isotopic values of AP, NOF, NHF, SON, and S&M were considered, whereas NO_3-based desert deposits were excluded, as the study area is located in the Mediterranean region. As the present study does not cover large number of water samples analyzed for nitrate isotopes (n = 17), the end-member isotopic values of the different potential sources of NO_3 were adopted from Torres-Martínez et al. (2021), who investigated NO_3 contamination in an area with comparable NO_3 anthropogenic sources. The $\delta^{15}N_{NO3}$ end-member isotopic values are: 0.11±1.69‰ for AP; −0.07±2.85 for NOF, 1.24±1.44‰ for NHF, 3.26±1.99‰ for SON, and 10.14±4.53‰ for S&M. The $\delta^{18}O_{NO3}$ end-member isotopic values are: 54.97±7.63‰ for AP, 24.12±3.17‰ for NOF, 3.44±2.47‰ for NHF, 3.34±2.04‰ for SON; and 5.69±2.91‰ for S&M.

4 Results and discussions

4.1 General overview on water quality

The analytical results of the chemical concentrations concerning the water samples collected over the study area are presented in Table 1. Groundwater from the study area is circumneutral with pH values varying from 6.3 to 7.7 without significant spatial variation. Groundwater displayed EC values ranging from 303 to 1,178 µS/cm with a median value of 619 µS/cm; the elevated EC values of 1,178 µS/cm (well #16), 1,004 µS/cm (well #15), and 861 µS/cm (well #22) correspond, respectively, to the urbanized sectors of Dem El-Begrat, Ben-Azouz, and Zaouia, suggesting an active mineralization potentially derived

from urban anthropogenic sources. All groundwater samples revealed acceptable concentrations in SO_4 relative to the respective drinking water limit of 500 mg/L that is recommended by the World Health Organization (WHO, 2017). Also, groundwater samples showed low concentrations of NH_4 with values below a maximum of 0.5 mg/L. Three groundwater samples (#15, #16, and #22) revealed Mg concentrations exceeding a value of 30 mg/L. However, the set of the collected groundwater samples have a median Mg concentration of 11.32 mg/L. High concentrations were identified for the other major elements including HCO_3 (max. = 433 mg/L, median = 223 mg/L), Cl (max. = 151 mg/L, median = 62.1 mg/L), Na (max. = 86.3 mg/L, median = 51.4 mg/L), K (max. 26.8 mg/L, median = 7.66 mg/L), and Ca (max. 120.3 mg/L, median = 51.4 mg/L). In groundwater, NO_3 concentrations were detected with values ranging from 2.8 to 166 mg/L. Nine groundwater samples revealed NO_3 concentration above the natural baseline threshold value of 5 mg/L (Appelo and Postma, 2005; Panno et al., 2006), suggesting potential anthropogenic influence over the study area. Surface water samples revealed a median pH value of 7.1. Excessive NH_4 concentrations were observed for some surface water samples (#13 = 22.3 mg/L; #14 = 16.3 mg/L) suggesting an anthropogenic influence. The surface water samples show a cationic dominance of Na (median value of 132 mg/L) or Ca (median value of 75.5 mg/L); the other major cations are ranked as follow Mg > K > NH_4 with corresponding median values of 27.8, 11.1, and 0.1 mg/L, respectively. For anions, Cl exhibited the highest concentrations with median value of 249 mg/L, whereas the other major anions are ranked as follow regarding their concentrations: HCO_3 > SO_4 > NO_3, with respective median values of 175, 47.1, and 8.2 mg/L. Nitrate concentrations from the collected surface waters ranged from 0.4 to 75.9 mg/L.

Table 1. Major chemical concentrations and stable isotope compositions of groundwater and surface water samples.

Sample ID	Water type	pH	T (°C)	EC (µs/cm)	TDS (mg/L)	HCO_3^- (mg/L)	Cl^- (mg/L)	Br^- (mg/L)	NO_3^- (mg/L)	SO_4^{2-} (mg/L)	Na^+ (mg/L)	NH_4^+ (mg/L)	K^+ (mg/L)	Mg^{2+} (mg/L)	Ca^{2+} (mg/L)	IBE (%)	δ^2H_{H2O} (‰)	$\delta^{18}O_{H2O}$ (‰)	d-excess (‰)*	$\delta^{15}N_{NO3}$ (‰)	$\delta^{18}O_{NO3}$ (‰)	^3H (TU)
#1	SW	7.73	15.30	1744	1106	87.84	613.23	2.10	2.09	38.39	252.74	0.12	6.00	44.32	58.79	-5	13.5	3.01	-10.59	5.4	21.5	3.0±0.3
#2	SW	7.18	17.19	976	606	151.28	244.32	0.96	0.39	16.61	122.56	0.04	9.05	21.65	38.95	-2	11.4	3.52	-16.69	-2.4	35.3	3.3±0.3
#3	SW	7.11	17.66	2485	1435	148.84	660.41	2.52	1.83	122.39	360.41	b.d.l	5.19	58.71	74.89	+1	4.7	1.66	-8.57	18.7	11.3	-
#4	SW	6.80	17.85	1427	9087	267.18	4700.58	18.69	14.04	692.07	2802.56	b.d.l	93.68	324.27	174.18	+2	-11.5	-1.89	3.64	7.1	3.0	-
#5	SW	6.65	15.80	1373	911	295.24	185.45	0.58	62.61	118.83	103.69	b.d.l	11.65	29.54	103.12	-5	-18.8	-3.02	5.31	8.9	6.1	-
#6	SW	7.57	19.97	860	618	198.86	101.76	0.39	0.55	138.32	71.52	0.32	9.91	16.82	80.00	-2	-19.8	-3.47	8.01	0.8	26.0	2.3±0.2
#7	SW	8.22	18.17	308	249	92.72	42.41	0.16	30.84	16.50	26.22	0.00	1.76	5.96	32.10	-4	-31.5	-5.73	14.36	-	-	1.7±0.2
#8	SW	7.03	14.88	1314	881	118.34	313.88	0.83	3.17	180.81	140.66	0.10	8.60	32.68	81.97	-5	-7.9	-1.07	0.69	12.5	3.9	-
#9	SW	6.75	14.84	1205	759	98.82	343.97	1.59	8.95	39.25	181.86	0.09	13.42	19.91	51.16	0	22.0	5.35	-20.79	-	-	-
#10	SW	6.75	16.39	1349	954	335.5	253.56	0.71	64.27	14.01	157.09	b.d.l	29.27	20.87	79.20	-3	-	-	-	-	-	1.8±0.2
#11	SW	7.62	17.02	1295	875	231.8	311.32	1.04	7.45	54.97	169.60	1.05	24.60	33.31	39.41	-4	15.4	3.95	-16.19	-	-	3.0±0.2
#12	SW	7.88	16.08	380	270	104.92	59.82	0.22	1.43	24.16	30.75	0.05	10.46	10.51	28.05	-1	-22.5	-3.61	6.41	-	-	-
#13	SW	6.48	17.02	1080	769	276.94	140.87	0.36	75.92	39.11	97.21	22.28	14.08	25.98	76.08	+5	-23.6	-4.27	10.56	0.5	3.8	-
#14	SW	6.25	15.88	1287	907	256.2	195.73	0.56	69.50	116.07	105.43	16.35	12.57	30.28	104.69	+1	-23.4	-3.66	5.94	2.8	4.8	-
#15	GW	7.44	17.71	1004	799	433.1	76.08	0.56	18.39	51.69	58.43	0.03	0.87	39.18	120.31	+5	-32.8	-5.83	13.79	2.3	29.8	-
#16	GW	6.93	20.77	1178	941	278.16	150.75	0.44	166.01	92.10	86.26	0.05	26.83	36.58	103.59	-3	-33.0	-6.08	15.64	-	-	-
#17	GW	7.51	21.20	303	247	74.42	48.72	0.16	44.23	9.85	22.92	b.d.l	7.93	4.79	34.34	-3	-25.5	-4.58	11.12	13.7	14.3	-
#18	GW	7.57	17.4	311	258	137.86	18.72	0.08	15.93	9.42	13.17	0.03	26.54	3.18	32.97	-1	-27.8	-4.91	11.51	1.1	27.0	2.7±0.3
#19	GW	6.40	21.75	417	314	57.34	60.49	0.36	79.91	32.55	29.71	b.d.l	5.22	11.12	37.61	-5	-27.2	-5.24	14.67	5.2	6.0	-
#20	GW	7.66	22.49	394	284	42.7	45.83	0.15	86.22	30.17	28.93	0.00	17.54	8.49	24.27	-5	-26.6	-4.97	13.14	4.5	9.4	-
#21	GW	7.27	19.28	640	534	264.74	83.99	0.3	2.79	34.46	58.37	0.51	14.65	8.72	65.19	-4	-31.8	-5.88	15.25	-1.1	22.2	-
#22	GW	7.57	21.14	861	717	296.46	63.63	0.28	119.33	55.33	67.08	0.03	7.40	31.76	75.43	-1	-23.7	-4.45	11.93	-	-	-
#23	GW	6.26	18.43	720	544	223.26	124.28	0.44	7.36	32.31	70.91	0.04	6.19	12.66	66.40	-2	-28.2	-5.10	12.57	14.2	4.3	-
#24	GW	7.39	20.01	366	285	93.94	53.70	0.21	32.88	29.57	44.37	b.d.l	0.79	11.51	18.18	-5	-30.0	-5.39	13.19	8.5	4.9	-
#25	MS	6.46	19.46	47620	37357	165.92	20850.63	73.95	21.38	2757.80	11410.75	b.d.l	383.33	1294.64	398.92	-1	1.7	0.46	-1.94	-	-	-
#26	RW	-	-	-	-	-	131.08	-	23.82	6.43	68.19	0.3	1.58	1.07	11.6	-	-	-	-	-	-	-

SW : Surface water
GW : Groundwater
RW : Rainwater
MS : Mediterranean Sea
b.d.l : below detection limit
IBE : Ionic balance error
- : No analysis
*: D-excess is computed as follows: d-excess = $\delta^2H_{H2O} - 8\delta^{18}O_{H2O}$

4.2 **Nitrate contamination**

4.2.1 Nitrate distribution over the study area

Figure 4 shows that groundwater featuring NO_3 concentrations above the WHO drinking water guideline (NO_3 >50 mg/L) correspond to rural communities of Dem El-Bagrat (#16), El-Guelb (#19), Marabout Aïcha (#20), and the village of Zaouia (#22), suggesting a potential urban influence. Groundwater samples #17 and #24, collected from private wells located in small villages, revealed moderate concentrations in NO_3 (30 mg/L< NO_3 <50 mg/L), whereas those having NO_3 concentrations <30 mg/L (#15, #18, #21 and #23) correspond to the less urbanized sector. Nitrate concentrations are not continuously monitored over the study area, but the maximum NO_3 concentration in groundwater (up to 97 mg/L) detected in 2007 (Hadj-Said, 2007) is lower than the maximum value of 166 mg/L reported in the present study. Figure 4 shows that NO_3 >50 mg/L in surface waters occur in the southern part of the study area, including one sample (#13) collected from Magroune SWS, two samples (#5 and #14) from the upstream of El-Kebir River, and one sample (#10) from Ain-Nechema SWS, which is connected to the El-Kebir River. Nitrate concentrations along the El-Kebir River decrease from >60 mg/L to 14 mg/L with flow downstream, indicating either dilution or denitrification.

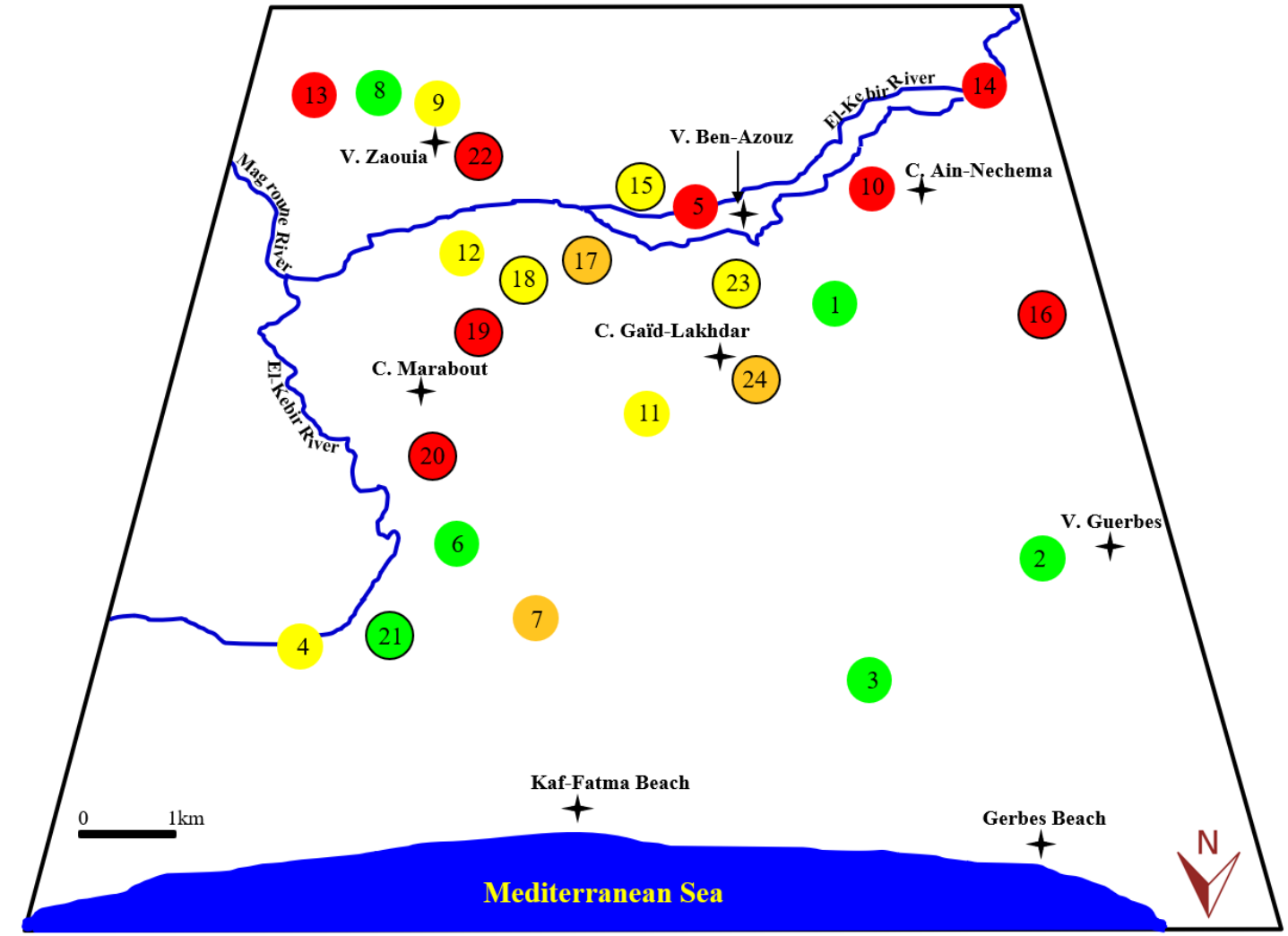

NO_3 >50 mg/L 30 mg/L< NO_3 <50 mg/L 5 mg/L< NO_3 <30 mg/L NO_3 <5 mg/L Groundwater

Figure 4. Spatial distribution of NO_3 concentrations over the study area.

4.2.2 Sources and apportionment of nitrate in water systems

Groundwater have $\delta^{15}N_{NO3}$ values ranging from −1.1‰ to 14.2‰ with a median value of 4.9‰; and $\delta^{18}O_{NO3}$ values varying between 4.3‰ and 29.8‰ with a median value of 11.8‰. Surface water samples have values ranging from −2.4‰ to 18.7‰ with a median value of 5.4‰ for $\delta^{15}N_{NO3}$; and from 3‰ to 35.3‰ with a median value of 6.1‰ for $\delta^{18}O_{NO3}$ (Table 1). Result from Kendall's diagram indicates that the study area is affected by multiple sources of NO_3 (Figure 5a). Groundwater samples fall within two main groups. The first one contains groundwater samples plotting in the manure and sewage zone (Figure 5a), including two groundwater samples (#19 and #20) with nitrate isotopic compositions that plot in the overlapping area of manure and sewage with soil-derived nitrogen. The second group contains groundwater samples falling within NO_3-based atmospheric precipitation including one groundwater sample (#21) having nitrate isotopic values falling in the overlapping area of NO_3-based atmospheric precipitation and NO_3-based fertilizers. Similarly, surface water samples fall in two groups identified for groundwater; except surface water sample #13 that plots in the overlapping area of manure and sewage with NH_4-fertilisers, and #1 having nitrate isotopic values falling in the overlapping area of NO_3-based atmospheric precipitation and NO_3-based fertilizers (Figure 5a).

The combined analysis of $\delta^{15}N_{NO3}$ and $\delta^{18}O_{NO3}$ makes it possible to evaluate nitrate transformation processes in a water system subjected to microbial denitrification (Böttcher et al., 1990; Wassenaar, 1995). Specifically, the denitrification process is commonly reflected by a positive 2:1 relationship between $\delta^{15}N_{NO3}$ and $\delta^{18}O_{NO3}$ (Mengis et al., 1999; Singleton et al., 2007). Here, the scattered distribution of $\delta^{15}N_{NO3}$ and $\delta^{18}O_{NO3}$ (Figure 5a) makes it difficult to distinguish between mixing of differently denitrified sources and actual

denitrification. The MixSIAR model results (Figures 5b, c) suggest that sewage and manure (S&M) are the main NO_3 sources both in groundwater (31.7%) and surface water (29.6%); a finding which is consistent with the above outcomes from Kendall's diagram. The other considered sources of NO_3 in groundwater are observed with the following ranking order: SON=20.1%, AP=18%, NOF=15.5%, NHF=14.7% (Figure 5b). In surface water, these sources are ranked as follow SON=21.1%, NOF=17.8%, AP=17.1%, NHF=14.4% (Figure 5c).

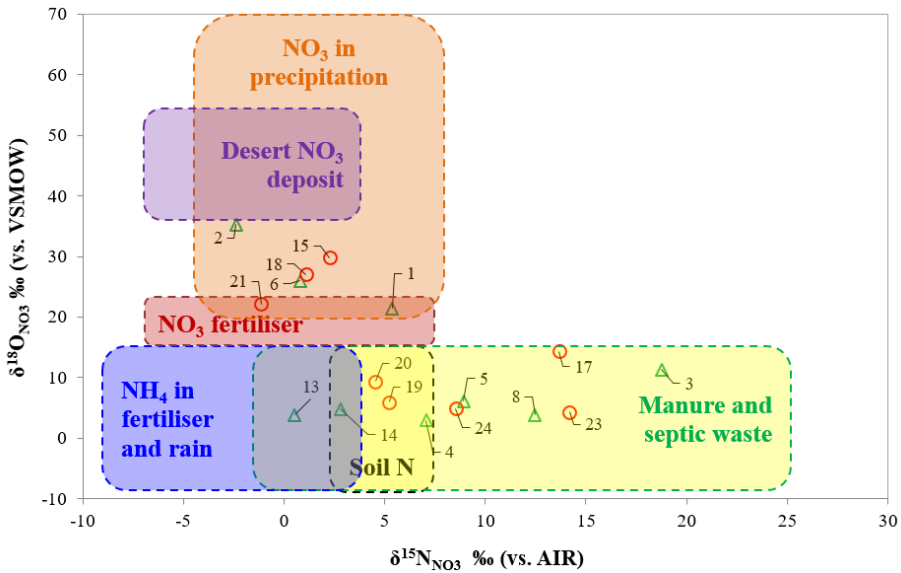

(a)

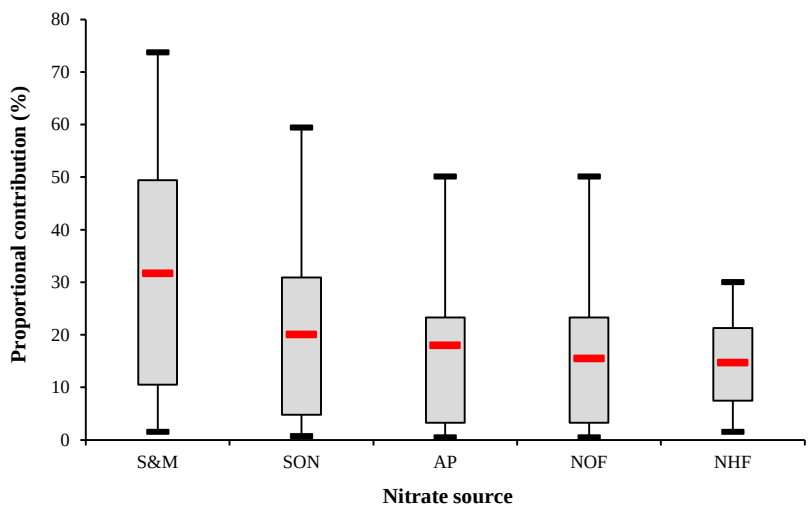

(b)

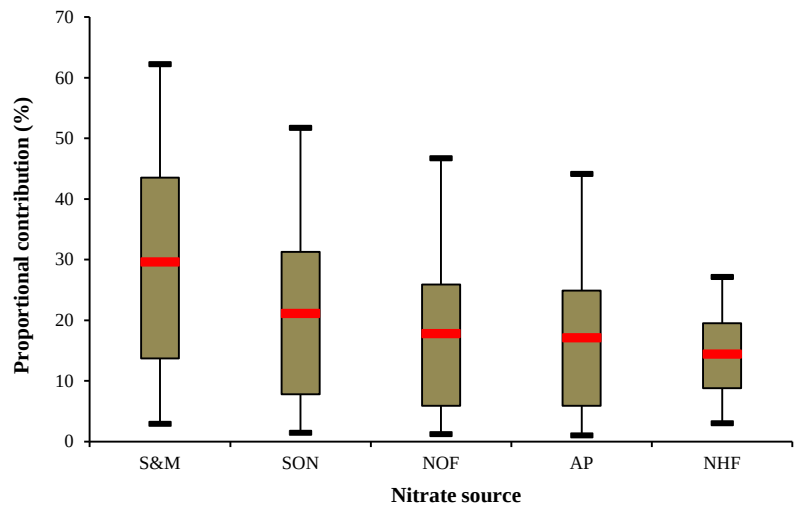

(c)

Figure 5. (a) Plot of $\delta^{15}N_{NO3}$ versus $\delta^{18}O_{NO3}$ values on Kendall's diagram; (b) apportionment of NO_3 sources in groundwater; and (c) apportionment of NO_3 sources in surface water. In (a), red circle indicates groundwater sample, whereas green triangle displays surface water sample. In (b) and (c), boxplots illustrate the 25th, 50th, and 75th percentiles, whereas the whiskers indicate 5th and 95th percentiles. S&M: sewage and manure, SON: soil organic nitrogen, AP: NO_3-based atmospheric precipitation, NOF: NO_3-based fertilizers, NHF: NH_4-fertilizers.

4.2.3 Discussion on the sources of nitrate

It is somewhat surprising that S&M are identified as the main sources of NO_3 over the study area, because previous studies (e.g., Hadj-Said, 2007) assumed synthetic fertilizers as the main NO_3 source. Nitrate derived from sewage within the study area could be from two sources. First, NO_3 could be derived from inefficient private sanitation systems still used by rural residences that are unable to connect to the collective sanitation networks. These inefficient private sanitation systems are commonly built with open-bottom sewage storage through which wastewater can directly reach groundwater (Boumaiza et al., 2021b, 2020, 2019). Second, NO_3 could be derived from wastewater discharge from sanitation networks as the El-Kebir River, which crosses the study area, receives wastewater discharges without pre-treatment (Bouleknafet and Derradji, 2017; Toubal et al., 2014). Likely, these wastewater discharges explain the concentrations of NO_3 detected from surface water samples collected from the El-Kebir River. Nitrate derived from manure source within the study area are linked to animal manure that is applied as an organic fertilizer. Further investigations based on additional isotope tracers and/or emerging compounds could help to distinguish sewage from animal waste source (Erostate et al., 2019; Lasagna and De Luca, 2017). Using animal manure to fertilize crops in agricultural areas is a common practice in Algeria because the use of industrial synthetic fertilizers has been prohibited by the Algerian Government since the 1990s (Chabour, 2004). Surface water samples #1 and #21, having nitrate isotopic values falling in the overlapping area of NO_3-based atmospheric precipitation and NO_3-based fertilizers (Figure 5a), could be accordingly assumed to have NO_3-based atmospheric precipitation source.

The accumulation of NHF, SON, and NOF in water systems of the study area agrees with land use, which has been traditionally dominated by agricultural activities. Detecting NO_3 contributions derived from NHF, SON, and NOF in groundwater corresponds to what could be expected for the unconfined aquifer of the study area, which is mainly dominated by sandy material with high permeability. Such material allows the infiltration of leached NO_3-based fertilizers, which could occur via: (i) direct rainwater infiltration and/or during irrigation water-return that subsequently facilitates the leaching of fertilizers added on the agricultural lands, and/or (ii) via potential NO_3-impacted surface water influx (Malki et al., 2017; Zhang et al., 2014).

Although the majority of emitted anthropogenic nitrogen components can enter terrestrial and marine ecosystems via atmospheric nitrogen deposition (Galloway et al., 2008), a potential NO_3-based atmospheric precipitation influence was neglected in previous studies undertaken in the study area (Bouleknafet and Derradji, 2017; Hadj-Said, 2007; Hedjal et al., 2018; Toubal et al., 2014). The present study identifies NO_3-based AP with a high apportionment both in groundwater (18%) and surface water (17.1%). This finding shows the particular features of the study area experiencing multi-anthropogenic sources of NO_3, compared to other recent studies on Algerian coastal areas that did not reveal NO_3-based atmospheric precipitation influence (Boumaiza et al., 2022, 2020). In the present study, the AP apportionment in groundwater is higher than those of NOF (15.5%) and NHF (14.7%), whereas in surface water it is higher than NHF (14.4%) and showed comparable apportionment to that of NOF (17.8%). This finding illustrates the significant influence of atmospheric precipitation on the NO_3 concentrations and agrees with high NO_3 concentration measured in the collected rainwater sample (23.8 mg/L; sample #26 in Table

1). While there is no on-going monitoring of NO_3 concentration in rainwater within the study region, the measured concentration of NO_3 in rainwater from this study is about eight times greater than that measured by Erostate et al. (2018), who studied a proximal Western Mediterranean coastal ecosystem. The present study also reveals that AP apportionments in groundwater (18%) and surface water (17.1%) are relatively high compared to other agricultural areas where contributions from AP did not exceed 4% (He et al., 2022; Li et al., 2022; Torres-Martínez et al., 2021).

Recent environmental studies demonstrated the presence of atmospheric nitrogen from anthropogenic sources across regions neighbouring the study area (Mourdi, 2011; Nadhir, 2019). However, these studies did not distinguish the impact of atmospheric nitrogen on groundwater resources as demonstrated in the present study. Further specific local studies are recommended to investigate the potential sources of atmospheric nitrogen within the study area. The Kendall diagram (Figure 5a) shows that surface water samples (#1, #2, and #6) and groundwater samples (#15, #18, and #21) —that are impacted by NO_3-atmospheric precipitation— are distributed relatively evenly over the entire study area (Figure 4). Accordingly, potential migration of NO_3-impacted water could occur via interactions between surface water and groundwater, which justifies our second objective to identify these potential interactions within the study area. The increase in nutrient inputs, enhanced by urban, agricultural, or industrial discharges not only impact groundwater quality, but can also upset the biodiversity equilibrium of ecosystems, causing ecological damages that result in deterioration of ecosystem functions, and consequently, diminishing profitable benefits of these ecosystems (Erostate et al., 2022; García and Muñoz-Vera, 2015).

4.3 Groundwater/surface water origin and interactions

4.3.1 Water origin and potential salinization processes

The δ^2H_{H2O} and $\delta^{18}O_{H2O}$ compositions as well as ^3H activities for the samples drawn from groundwater and surface water from the study area are presented in Table 1. The isotopic compositions of the groundwater samples range from −6.1‰ to −4.5‰ for $\delta^{18}O_{H2O}$; and from −33‰ to −23.8‰ for δ^2H_{H2O}; these groundwater isotopic values are comparable to other North-Africa Mediterranean coastal aquifers (Boumaiza et al., 2022, 2020; Chafouq et al., 2018; Elmeknassi et al., 2022). The surface water samples revealed isotopic compositions ranging from −5.7‰ to +5.3 for $\delta^{18}O_{H2O}$; and from −31.5‰ to +22‰ for δ^2H_{H2O}. The Mediterranean Sea sample displays isotopic values corresponding to −0.46‰ for $\delta^{18}O_{H2O}$ and 1.7‰ for δ^2H_{H2O}. In the present study, the $\delta^{18}O_{H2O}$ and δ^2H_{H2O} values are interpreted according to the Global Meteoric Water Line (GMWL) (Craig, 1961) and the Western Mediterranean Meteoric Water Line (WMMWL) (Celle, 2000). In Figure 6, groundwater samples cluster around the WMMWL suggesting that the groundwater has been recharged into the aquifer through direct infiltration of rainwater with minimal evaporation. This corresponds to what could be expected for the unconfined aquifer of the study area composed of permeable sediments. The groundwater d-excess values, ranging from +11.12 to +15.64‰ (Table 1), are indicative of modern recharge having typical isotopic compositions of recharge derived from Mediterranean moisture sources (Celle-Jeanton et al., 2001; Gat and Carmi, 1970). The range of the calculated groundwater d-excess can be explained by mixing processes involving local groundwater with other groundwater having different isotopic signatures (Tantawi et al., 1998). The mixing process is evidenced also by isotopic enrichment directed towards the Mediterranean Sea isotopic

signature (blue point in Figure 6). However, this isotopic enrichment could constitute the result of infiltrated evaporative water, like infiltrated rainwater affected by evaporation during precipitation events (Clark and Fritz, 1997). Other studies in Algeria have noted evaporative rainwater with comparable slope to that obtained in the present study (Mebrouk et al., 2007; Moulla and Guendouz, 1996). Nonetheless, as the groundwater samples fall above the GMWL, mixing process is rather expected.

Most surface water samples display heavier isotopic values compared to those of groundwater and deviate from the GMWL by following a distinct line (Figure 6) indicating a high isotopic fractionation effect. The latter feature could be related to a high evaporation effect because (i) the evaporation line falls below the seawater mixing line, and (ii) the d-excess displays low values (Boumaiza et al., 2021a; Gemitzi et al., 2014). In Figure 7, slight positive correlation is observed between surface water Cl and $\delta^{18}O_{H2O}$ values (R^2 = 0.6) suggesting an increase in salinity accompanying heavy isotope enrichment. This positive relationship confirms the above effect of the evaporation process. Samples from El-Kebir River (#4, #5, and #14) display an isotopic enrichment towards the downstream direction of water flow with respective d-excess values of 5.94‰ (#14), 5.31‰ (#5), and 3.64‰ (#4). The water along the El-Kebir River is mostly controlled by the Bekouche-Lakhdar Dam —implemented at an upstream level of the El-Kebir River— which decreases the flow along the El-Kebir River, leading to more surface water evaporation (Toubal et al., 2014). This can explain why surface water samples #4, #5, and #14 from the El-Kebir River show isotope evidence of evaporation. However, mixing is also probable, particularly for sample #4, which plots along the seawater mixing line.

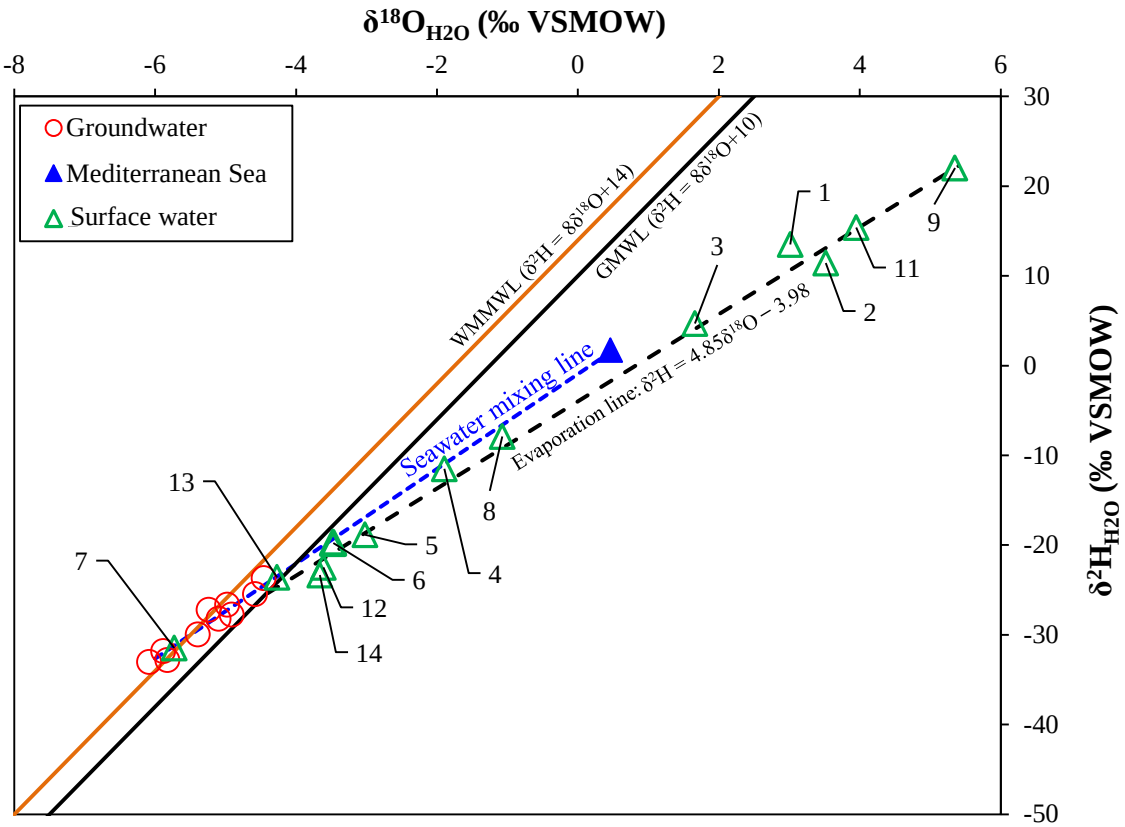

Figure 6. Distribution of $\delta^{18}O_{H2O}$ and $\delta^{2}H_{H2O}$ isotopic compositions of the collected groundwater and surface water samples.

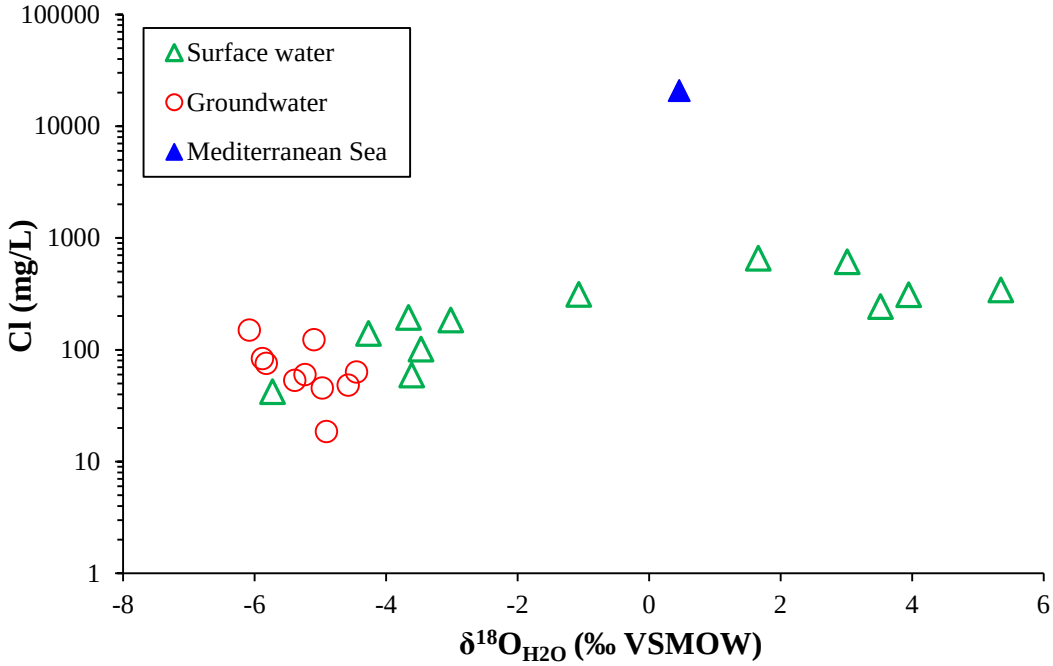

Figure 7. Plot of $\delta^{18}O_{H2O}$ isotopic values versus Cl-groundwater

4.3.2 Dominant water type for groundwater and surface water

The plot of the ten collected groundwater samples on the Piper diagram (Figure 8a) shows the dominance of two main water types. Four groundwater samples (#15, #18, #21, and #22) are dominated by Ca-HCO_3 water type, whereas the other samples (#16, #17, #19, #20, #23, and #24) plot within the field of the Ca-Cl mixed water type. Wells #15, #18, and #22 potentially correspond to a recharge area as they are characterized by a classic Ca-HCO_3 water type, which is indicative of recent recharge (Hiscock, 2009). Well #21 is located downhill from the sandy dune deposits occupying the northeastern part of the study area. The presence of Ca-HCO_3 water type at well #21 could also reflect recent recharge through the sandy dune deposits. Freshening of groundwater from wells #15, #18, #21, and #22 is supported by the Gibbs's diagram (Figure 8c), which shows that these samples form a distinct group that have been impacted by the freshening process. The other six groundwater samples (#16, #17, #19, #20, #23, and #24), which plot as Ca-Cl mixed water type on the Piper diagram, are distributed over the central part of the study area (Figure 9), with samples #16, #23, and #24 located towards the east, and the samples #17, #19, and #20 situated towards the west of the study area. The Gibbs's diagram (Figure 8c) suggests that samples #17, #19, and #20 are predominantly undergoing a freshening process, whereas samples #16, #23, and #24 are undergoing mixing process. It is possible that Ca-HCO_3 water type, identified at wells #15 and #18 experienced some freshening control on groundwater at wells #17, #19, and #20, resulting in the mixed water type described above. The Cl concentrations presented in Table 1 show that highest Cl and Na concentrations occur in groundwater from well #16 (Cl = 151 mg/L; Na = 86.3 mg/L) and well #23 (Cl = 124 mg/L; Na = 70.9 mg/L). These two inland wells are located far from the Mediterranean

Sea shoreline (Figure 3). Conversely, groundwater from well #21, neighboring the Mediterranean Sea, revealed low concentrations in Cl (83.9 mg/L) and Na (58.4 mg/L). These patterns of Cl concentrations suggest that groundwater from wells #16 and #23 is enriched in Cl and Na from other potential sources rather than direct enrichment from the Mediterranean Sea. The fact that groundwater from wells #15, #22, and #24 plot below the equiline of 1:1 on Figure 8d indicates slight dominance of Na over Cl. Calcium exchange from freshwater (Ca-HCO_3 in composition) with Na sorbed on clays minerals is a common process along groundwater flow paths (Lee, 1985; Park et al., 2009; Toran and Saunders, 1999). The consequence of this cationic exchange process is an increase in Na concentration in groundwater, which is commonly observed in coastal aquifers (Appelo and Postma, 2005). However, we cannot exclude the possible influence of an anthropogenic source of Na (e.g., urban wastewater) as the samples #15, #22, and #24 were collected from urbanized sectors of the study area.

The two surface water samples collected along upstream portions of the El-Kebir River (#14) and Ben-Azouz (#5) correspond to the Ca-Cl mixed water type, whereas the sample collected from the downstream of the El-Kebir River (#4) corresponds to the Na-Cl water type. This observation suggests surface water evolution as water flows downstream; also, there is potential high mixing of surface water at sampling point #4 with the Mediterranean Sea as the El-Kebir River (sample #4) is connected to the Mediterranean Sea. We note that river water samples from the downstream portion of the El-Kebir River exhibit a similar signature to that of the Mediterranean Sea on the Piper diagram (Figure 8b). Mixing of El-Kebir River waters with the Mediterranean Sea is also supported by the Gibbs diagram (Figure 8c), on which the downstream El-Kebir River water sample plots

within a region suggestive of mixing with the Mediterranean Sea. The Piper diagram shows that surface water samples are dominated by saline waters of the Na-Cl type as well as mixed water of the Ca-Cl type. These two water types are also evidenced by the Gibbs diagram (Figure 8c), wherein the water surface samples having Na-Cl water type (#1, #2, #3, #4, #9, #10, and #11) plot in advanced mixing stage compared to those having mixed Ca-Cl water type (#5, #6, #7, #8, #12, #13, and #14) that are grouped in early mixing stage.

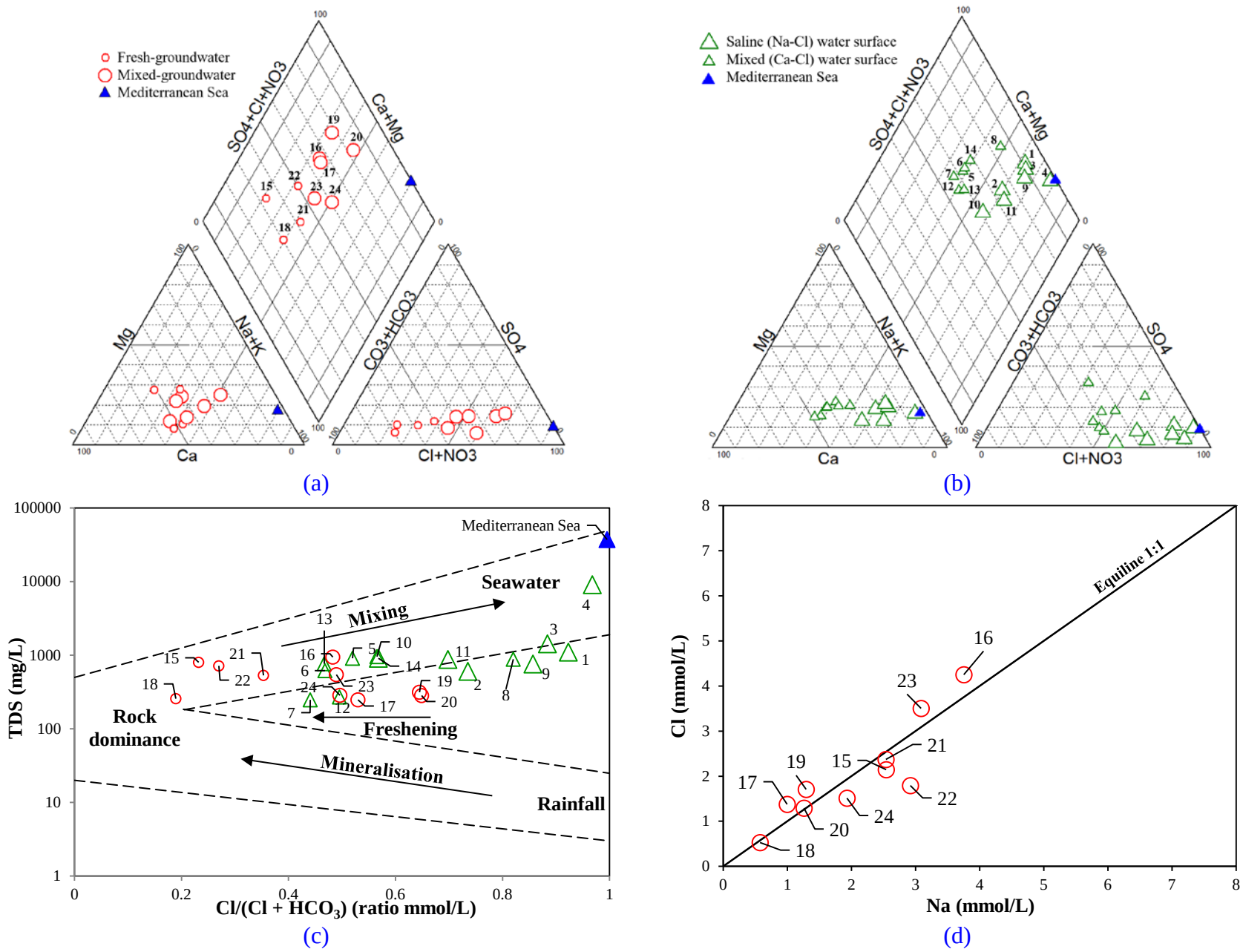

Figure 8: (a) Plot of groundwater samples on Piper's diagram; (b) Plot of surface water samples on Piper's diagram; (c) Plot of both groundwater and surface water samples on Gibbs's diagram; (d) Relationship between Na and Cl concentrations in groundwater.

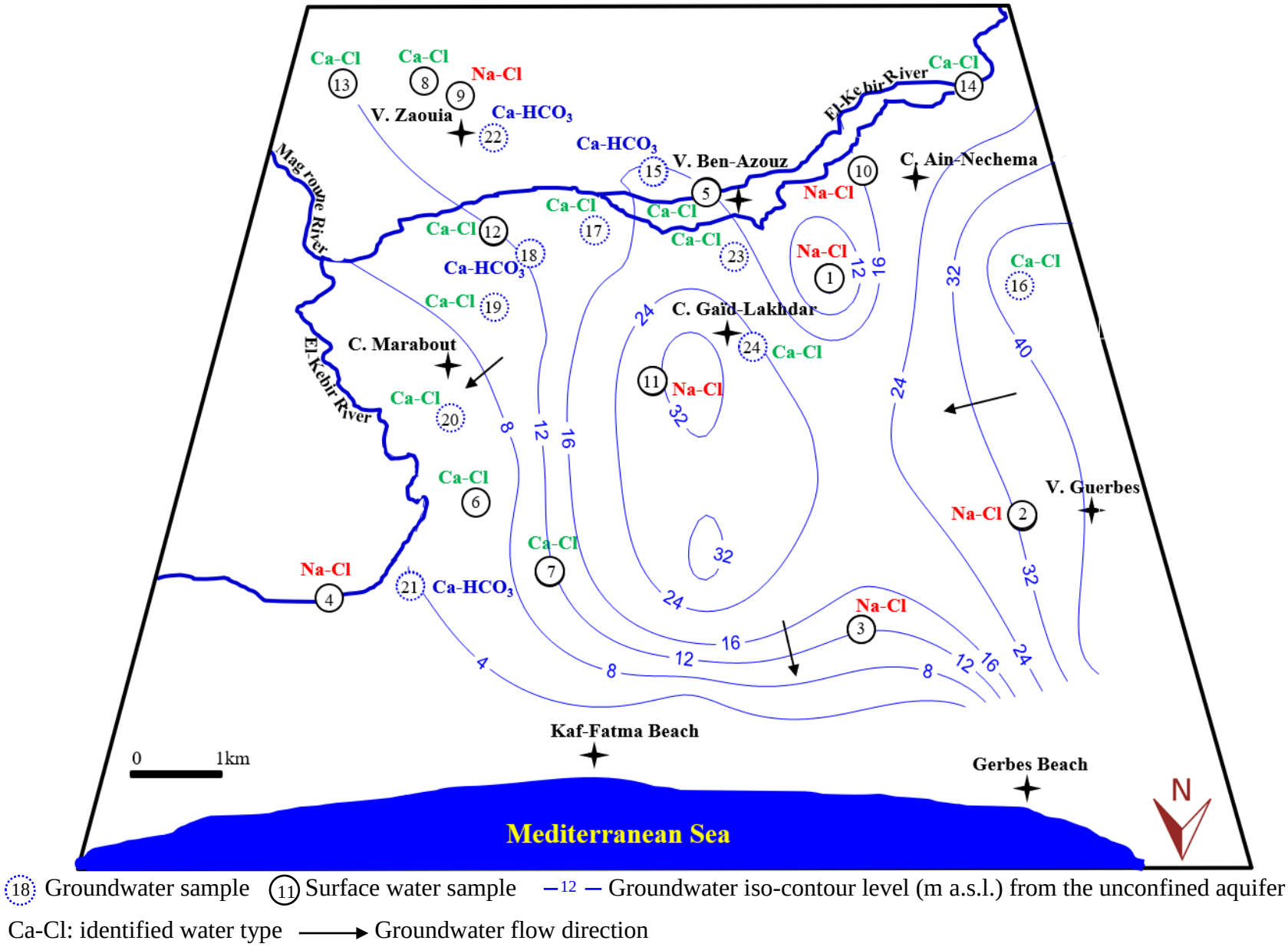

Figure 9. Distribution of water type over the study area. In bold-blue are Ca-HCO_3 water type, in bold-green are Ca-Cl water type, and in bold-red are Na-Cl water type.

4.3.3 Isotopic evidence of surface water/groundwater interactions

In Figure 6, surface water sample #7 falls on the WMMWL suggesting less evaporation effect, despite the fact that open surface water systems are commonly subjected to greater evaporation than groundwater (Dindane et al., 2003). Surface water sample #7 displayed a high d-excess value of 14.4‰ and also plots on seawater mixing line. These observations suggest that surface water is subject to mixing process, which can also explain why sample #7 is classified as a Ca-Cl mixed water type according to the Piper diagram. The mixing process is also evidenced from the ^{3}H content. Here, the surface water sample #7 revealed ^{3}H content of 1.7±0.2 TU, indicating a reduced activity relative to the rainwater ^{3}H content having weighted mean of 3.8 TU (Erostate et al. 2018). Hence, surface water sample #7 must have mixed with older water. Moreover, surface water sample #7 exhibits an isotopic signature within the range of the groundwater samples (Figure 6), confirming that surface water from site #7 likely interacted with groundwater. Hence, potential migration of the identified NO_3-impacted water at site #7 (Figure 4) could occur via the evidenced interactions between surface water and groundwater. Surface water sample #13 collected from the Magroune SWS has $\delta^{18}O_{H2O}$ (−4.3‰) and $\delta^{2}H_{H2O}$ (−23.6‰) values that fall outside the range exhibited by the groundwater samples (Figure 6), and plots on both the GMWL and the seawater mixing line. These features suggest that sample #13 has experienced less evaporation while also undergoing possible mixing with saltwater, which agrees with the Piper diagram as sample #13 is classified as a Ca-Cl mixed water type. It appears that excessive pumping of water from the Magroune SWS, for irrigating the large neighbouring agricultural areas, has exerted some control on the isotopic features. When surface water is pumped from the Magroune SWS, the extracted water appears to include

a groundwater component because the isotopic signature of sample #13 is closer to that of the groundwater samples than to most of the surface water samples. Hence, the Magroune SWS appears to be a groundwater-dependent system containing less evaporated water due to the periodic pumping of its water. The Magroune SWS revealed elevated NO_3 concentration (75.9 mg/L), which suggests influence from manure and sewage sources that are evidenced by isotope of nitrate. Hence, mixing between the surface water and groundwater within the Magroune SWS, combined with the dependence of this SWS on groundwater, suggest that nitrate in the Magroune SWS is from groundwater impacted by manure and sewage inputs.

The two surface water samples #6 ($\delta^{18}O_{H2O} = -3.5‰$; $\delta^{2}H_{H2O} = -19.8‰$) and #12 ($\delta^{18}O_{H2O} = -3.6‰$; $\delta^{2}H_{H2O} = -22.5‰$), collected respectively from the Messoussa and El-Guelb SWSs, display comparable isotopic signatures. These two samples plot below the WMMWL and GMWL suggesting they were subject to evaporation process, which is also supported by their low d-excess values of 6.41‰ (#12) and 8.01‰ (#6). Sample #6 plots on the seawater mixing line, whereas sample #12 falls on the evaporation line; indicative of more evaporation from the El-Guelb SWS (#12) compared to the Messoussa SWS (#6). Sample #6 revealed a ^{3}H content (2.3±0.2 TU) that is lower than that of the local rainwater (3.8 TU), confirming that this surface water was subject to mixing processes with older groundwater. These observations further support the notion that the Messoussa SWS (#6) is a groundwater-dependent system, wherein its mixed Ca-Cl water type (Figure 9) results from groundwater-surface water interactions. Figure 9 shows that groundwater flow towards sample #6 is from an upstream zone where water is less affected by NO_3; reason

for which sample #6 revealed low NO_3 concentration (0.55 mg/L), which was distinguished to be with NO_3-based atmospheric precipitation origin.

Surface water samples #8 and #9 were collected from the Moussisi and Zaouia SWSs, respectively, both located at the southeastern part of the study area. These two samples fall on the evaporation line suggesting evaporation exerted some control on the surface water from both SWSs. However, sample #9 is more enriched in the heavy isotopes compared to sample #8 (Figure 6), leading to a d-excess value for sample #9 (−20.79‰) substantially lower than that of sample #8 (0.69‰). The Zaouia SWS (#9) is an isolated SWS; this type of isolated SWS is known to experience substantial evaporation (Kock et al., 2019) leading to evapo-concentrated water that explains the predominance of the Na-Cl water type (Figure 8). The Moussisi SWS is also isolated, but during flooding events becomes connected to the Magroune River. Hence, the Moussisi SWS drains excess water during these flooding events, which likely explains why it is dominated by less evapo-concentrated water of the Ca-Cl type. In the sector neighbouring the Moussisi and Zaouia SWSs, groundwater sample #22 revealed Ca-HCO_3 water type, wherein mineralization likely reflects mixing between meteoric Ca-HCO_3 water type —from the recharging area corresponding to well #22 featuring high groundwater level— and urban wastewater enriched in Cl. It is possible that the Cl concentrations measured in surface water samples #8 and #9 are partially derived from the mixing with groundwater, with some of the Cl content being concentrated by evaporation. High NO_3 concentration was measured in groundwater from well #22 (119 mg/L); this constitutes source of contamination that could be sprawled through the potential mixing process with groundwater. The mixing of groundwater in the south part of the study area is also supported by groundwater sample

#18, which exhibits a ^{3}H content of 2.7±0.3 TU that is lower than that of the local rainwater (3.8 TU). Figure 6 shows that surface water samples #1, #2, #3, and #11, collected respectively from the Hadj-Taher, Gerbes 1, Gerbes 2, and Gaïd-Lakhdar SWSs, plot along the evaporation line with enriched isotopic compositions. These surface water samples feature low d-excess values ranging from −16.2‰ to −8.6‰, suggesting they are predominantly affected by evaporation processes. However, they are not excluded from simultaneous mixing process. The water sample from the Hadj-Taher SWS, for example, shows evidence of strong evaporation (Figure 6), but it plots slightly off the evaporation line potentially due to mixing with saline water, as salinity is among the factors controlling the slope of the evaporation line (Gonfiantini et al., 2018; Tremblay et al., 2021). Furthermore, the samples #1, #2, and #11 have ^{3}H contents lower than that of the local rainwater (3.8 TU) suggesting mixing with older waters. This interpretation is also valid for the sample #10 collected from the Ain-Nechema SWS, which has a ^{3}H content of 1.8±0.2 TU. As the samples #1, #2, #3, #10, and #11 correspond to isolated SWSs, potential mixing with groundwater is expected. Hence, these SWSs constitute groundwater-dependent systems, involving active interactions between surface and groundwater, wherein potential migration of NO_3-impacted water from surface water to groundwater (and vice versa) is expected.

5 Conclusion

The effect of uncontrolled development strategies, over the Mediterranean coastal study site of Guerbes-Senhadja in Algeria, are reflected by elevated and harmful NO_3 concentrations. In fact, most of the detected NO_3 concentrations, both in groundwater and surface water, are above the WHO drinking water guideline or the natural baseline

threshold. Multiple sources of NO_3 were distinguished, wherein sewage and manure were observed to constitute the main sources of NO_3 in groundwater and surface water. It is somewhat surprising that sewage and manure constitute the chief sources of NO_3 as previous studies suggested, without using more conclusive isotopic tools, the use of synthetic fertilizers as the primary source contributing to the local nitrate pool. Here, NO_3 derived from manure sources is explained by the high amounts of additive animal manure used to fertilise the agricultural areas, whereas NO_3 derived from sewage source is related to rural wastewater discharge. The later can be sourced (i) from the private sanitation systems used by isolated residences that are unable to connect to the sanitation networks, and (ii) from the sanitation networks draining into the rivers without pre-treatment.

Compared to other recent studies on Algerian eastern coastal areas, the present study highlights the particular high apportionment of NO_3-based atmospheric precipitation —both in groundwater and surface water— agreeing with the high NO_3 concentration detected in rainwater. This new specific-site finding not only shows the particular features of the study area experiencing multiple sources of NO_3, but also demonstrates the effectiveness of using isotopic tracers to investigate the sources of nitrate in coastal ecosystems. Potential NO_3 from atmospheric precipitation was totally ignored in previous hydrogeological studies undertaken in the study area. However, this study did not identify the potential sources of NO_3 in local precipitation. Further efforts are recommended to monitor the NO_3 concentration in rainwater within the study area, and to investigate the relative sources of atmospheric nitrogen.

The present study revealed that NO_3-impacted groundwater/surface water samples are distributed relatively evenly over the entire study area. As the migration of NO_3-

impacted water could occur via interactions between surface water and groundwater; the present study highlights the identification of such interactions. Here, the evidenced interactions between surface water and groundwater, through using multi-isotopic tracers, suggest that surface water systems are dependent on groundwater and even groundwater within aquifer is dependent on surface water. This identified behavior over the study site shows the complex hydrogeology of this system, but provides helpful information to further local studies aiming to understand anthropogenic sprawl pathways within the entire Guerbes-Senhadja ecosystem. This potential research topic can be added to other researches focusing in developing environmental optimization strategies, to achieve a sustainable management of the Mediterranean coastal site of Guerbes-Senhadja, given the elevated NO_3 concentrations enhanced by multi-anthropogenic sources.

Acknowledgements

The authors thank Natural Sciences and Engineering Research Council of Canada that have funded this project (Grant number FGR-NSERC 326881 held by Prof. Julien Walter; and NSERC-Discovery Grand -RGPIN/07117- held by Prof. Romain Chesnaux). The authors also acknowledge the financial support from *Décanat de la recherche et de la création* of the *Université du Québec à Chicoutimi* (Grant number DGECR/00241-2021 held by Prof. Julien Walter). The authors thank the local population of Guerbes-Senhadja region (Algeria), who provided much relevant information about the management of their wastewater and offered free access to their private wells during fieldwork.

References

Appelo, C.A.J., Postma, D., 2005. Geochemistry, groundwater and pollution, second edition, Geochemistry, Groundwater and Pollution. 2nd Edition, Balkema, Leiden, The Netherlands.

Auzende, J.M., Bonnin, J., Olivet, J.L., 1975. La marge Nord-africainne considérée comme

marge active. Bull. la Société Géologique Fr. 7, 681–690.
Babouri, S., Metallaoui, S., Heddam, S., 2020. Abundance and spatial distribution of the structure supporting the nest ofWhite Stork Ciconia ciconia in Guerbes-Sanhadja wetland eco-complex, northeastern of Algeria. Environ. Sci. Pollut. Res. 27, 45974–45982.
Barhoumi, B., Le Menach, K., Clérandeau, C., Ben Ameur, W., Budzinski, H., Driss, M.R., Cachot, J., 2014. Assessment of pollution in the Bizerte lagoon (Tunisia) by the combined use of chemical and biochemical markers in mussels, Mytilus galloprovincialis. Mar. Pollut. Bull. 84, 379–390.
Barnes, R.S.K., 1980. Coastal Lagoons: The Natural History of a Neglected Habitat. Cambridge University Press, Cambridge.
Böttcher, J., Strebel, O., Voerkelius, S., Schmidt, H.L., 1990. Using isotope fractionation of nitrate-nitrogen and nitrate-oxygen for evaluation of microbial denitrification in a sandy aquifer. J. Hydrol. 114, 413–424.
Bouchaala, L., Elafri, A., Charchar, N., Boukhemza, M., Houhamdi, M., 2017. Wintering behaviour and spatial ecology of Eurasian Wigeon Anas penelope in a coastal Mediterranean wetland complex (Guerbes-Sanhadja) of northeastern Algeria. Avian Biol. Res. 10, 84–91.
Bouleknafet, Z., Derradji, E.F., 2017. Hydrogeology and Vulnerability to Pollution of the Water Resources in the Kebir West Plain. Rev. des Sci. la Technol. 34, 85–94.
Boumaiza, L., Chabour, N., Drias, T., 2019. Reviewing the potential anthropogenic sources of groundwater contamination - Case study of the expanding urban area of Taleza in Algeria, in: Proceedings of the 72nd Canadian Geotechnical Conference (GeoSt-John's 2019), Saint-John's, Newfoundland and Labrador, Canada,. p. 9.
Boumaiza, L., Chesnaux, R., Drias, T., Walter, J., Huneau, F., Garel, E., Knoeller, K., Stumpp, C., 2020. Identifying groundwater degradation sources in a Mediterranean coastal area experiencing significant multi-origin stresses. Sci. Total Environ. 746, 1–20.
Boumaiza, L., Chesnaux, R., Drias, T., Walter, J., Stumpp, C., 2021a. Using vadose-zone water stable isotope profiles for assessing groundwater recharge under different climatic conditions. Hydrol. Sci. J. https://doi.org/doi.org/10.1080/02626667.2021.1957479
Boumaiza, L., Chesnaux, R., Walter, J., Drias, T., Huneau, F., Garel, E., Vystavna, Y., Stumpp, C., 2021b. Reviewing the anthropogenic sources of groundwater contamination in the Plain of the El-Nil River, Algeria, in: Proceedings of the 74th Canadian Geotechnical Conference and the 14th Joint CGS/IAH-CNC Groundwater Conference (GeoNiagara-2021), Niagara Falls, Ontario, Canada. p. 9.
Boumaiza, L., Walter, J., Chesnaux, R., Zahi, F., Huneau, F., Garel, E., Stotler, R.L., Bordeleau, G., Drias, T., Johannesson, K.H., Vystavna, Y., Re, V., Knöller, K., Stumpp, C., 2022. Combined effects of seawater intrusion and nitrate contamination on groundwater in coastal agricultural areas: A case from the Plain of the El-Nil River (North-Eastern Algeria). Sci. Total Environ. 851, 1–13.
Boussehaba, A., 2010. Contribution to the ecological and cartographic study of the vegetation of the Sanhadja-Guerbes wetland complex. Master's thesis, Université d'Annaba, Algérie.
Camacho-Valdez, V., Ruiz-Luna, A., Ghermandi, A., Nunes, P.A.L.D., 2013. Valuation of

ecosystem services provided by coastal wetlands in northwest Mexico. Ocean Coast. Manag. 78, 1–11.

Cao, S., Fei, Y., Tian, X., Cui, X., Zhang, X., Yuan, R., Li, Y., 2021. Determining the origin and fate of nitrate in the Nanyang Basin, Central China, using environmental isotopes and the Bayesian mixing model. Environ. Sci. Pollut. Res. 28, 48343–48361.

Casciotti, K.L., Sigman, D.M., Hastings, M.G., Böhlke, J.K., Hilkert, A., 2002. Measurement of the oxygen isotopic composition of nitrate in seawater and freshwater using the denitrifier method. Anal. Chem. 74, 4905–4912.

Celle-Jeanton, H., Travi, Y., Blavoux, B., 2001. Isotopic typology of the precipitation in the Western Mediterrenean region at the three different time scales. Geophys. Res. Lett. 28, 1215–1218.

Celle, H., 2000. Caractérisation des précipitations sur le pourtour de la Méditerranée occidentale. Approche isotopique et chimique. PhD thesis, Université d'Avignon, France.

Chabour, N., 2004. La surexploitation des eaux souterraines dans les plaines littorales : la nappe de Télezza dans la plaine de Collo (Nord-Est algérien). Sci. Technol. 127–132.

Chafouq, D., El Mandour, A., Elgettafi, M., Himi, M., Chouikri, I., Casas, A., 2018. Hydrochemical and isotopic characterization of groundwater in the Ghis-Nekor plain (northern Morocco). J. African Earth Sci. 139, 1–13.

Clara, I., Dyack, B., Rolfe, J., Newton, A., Borg, D., Povilanskas, R., Brito, A.C., 2018. The value of coastal lagoons: Case study of recreation at the Ria de Aveiro, Portugal in comparison to the Coorong, Australia. J. Nat. Conserv. 43, 190–200.

Clark, I.D., Fritz, P., 1997. Environmental isotopes in hydrogeology. CRC Press-Lewis Publishers.

Cohen, C.R., 1980. Plate tectonic model for the oligo-miocene evolution of the western Mediterranean. Tectonophysics 68, 283–311.

Craig, H., 1961. Isotopic variations in meteoric waters. Science (80-.). 133, 1702–1703.

David, M., Bailly-Comte, V., Munaron, D., Fiandrino, A., Stieglitz, T.C., 2019. Groundwater discharge to coastal streams – A significant pathway for nitrogen inputs to a hypertrophic Mediterranean coastal lagoon. Sci. Total Environ. 677, 142–155.

Dindane, K., Bouchaou, L., Hsissou, Y., Krimissa, M., 2003. Hydrochemical and isotopic characteristics of groundwater in the Souss Upstream Basin, southwestern Morocco. J. African Earth Sci. 36, 315–327.

El Mahrad, B., Abalansa, S., Newton, A., Icely, J.D., Snoussi, M., Kacimi, I., 2020. Social-Environmental Analysis for the Management of Coastal Lagoons in North Africa. Front. Environ. Sci. 8, 1–17.

Elmeknassi, M., Bouchaou, L., El Mandour, A., Elgettafi, M., Himi, M., Casas, A., 2022. Multiple stable isotopes and geochemical approaches to elucidate groundwater salinity and contamination in the critical coastal zone: A case from the Bou-areg and Gareb aquifers (North-Eastern Morocco). Environ. Pollut. 300, 1–13.

Erostate, M., Ghiotti, S., Huneau, F., Jouffroy, D., Garel, E., Garrido, M., Pasqualini, V., 2022. The challenge of assessing the proper functioning conditions of coastal lagoons to improve their future management. Sci. Total Environ. 803, 1–10.

Erostate, M., Huneau, F., Garel, E., Ghiotti, S., Vystavna, Y., Garrido, M., Pasqualini, V., 2020. Groundwater dependent ecosystems in coastal Mediterranean regions: Characterization, challenges and management for their protection. Water Res. 172, 1–

19.
Erostate, M., Huneau, F., Garel, E., Lehmann, M.F., Kuhn, T., Aquilina, L., Vergnaud-Ayraud, V., Labasque, T., Santoni, S., Robert, S., Provitolo, D., Pasqualini, V., 2018. Delayed nitrate dispersion within a coastal aquifer provides constraints on land-use evolution and nitrate contamination in the past. Sci. Total Environ. 644, 928–940.
Erostate, M., Huneau, F., Garel, E., Vystavna, Y., Santoni, S., Pasqualini, V., 2019. Coupling isotope hydrology, geochemical tracers and emerging compounds to evaluate mixing processes and groundwater dependence of a highly anthropized coastal hydrosystem. J. Hydrol. 578, 1–22.
Galloway, J.N., Townsend, A.R., Erisman, J.W., Bekunda, M., Cai, Z., Freney, J.R., Martinelli, L.A., Seitzinger, S.P., Sutton, M.A., 2008. Transformation of the nitrogen cycle: Recent trends, questions, and potential solutions. Science (80-.). 320, 889–892.
García, G., Muñoz-Vera, A., 2015. Characterization and evolution of the sediments of a Mediterranean coastal lagoon located next to a former mining area. Mar. Pollut. Bull. 100, 249–263.
Gat, J.R., Carmi, I., 1970. Evolution of the isotopic composition of the atmospheric water in the Mediterranean Sea area. J. Geophys. Reseach 75, 3039–3048.
Gemitzi, A., Stefanopoulos, K., Schmidt, M., Richnow, H.H., 2014. Seawater intrusion into groundwater aquifer through a coastal lake - complex interaction characterised by water isotopes 2H and 18O. Isotopes Environ. Health Stud. 50, 74–87.
Gonfiantini, R., Wassenaar, L.I., Araguas-Araguas, L., Aggarwal, P.K., 2018. A unified Craig-Gordon isotope model of stable hydrogen and oxygen isotope fractionation during fresh or saltwater evaporation. Geochim. Cosmochim. Acta 235, 224–236.
Hadj-Said, S., 2007. Contribution à l'étude hydrogéologique d'un aquifère en zone côtière : cas de la nappe de Guerbès. Ph.D thesis, Université d'Annaba, Algérie.
He, S., Li, P., Su, F., Wang, D., Ren, X., 2022. Identification and apportionment of shallow groundwater nitrate pollution in Weining Plain, northwest China, using hydrochemical indices, nitrate stable isotopes, and the new Bayesian stable isotope mixing model (MixSIAR). Environ. Pollut. 298, 1–11.
Hedjal, S., 2019. Ressources en eau, gestion intégrée et perspectives d'un aménagement du complexe des zones humides de Guerbes (Nord Est algérien). Ph.D thesis, Université d'Annaba, Algérie.
Hedjal, S., Derradji, Z., Benamara, A., 2018. Hydrochemical assessment of water quality for irrigation: A case study of the wetland complex of Guerbes-Sanhadja, North-East of Algeria. J. Water L. Dev. 38, 43–52.
Hedjal, S., Derradji, Z., Benamara, A., Dandane, H., 2019. Essay of integrated water management of the wetland complex of Sanhadja (North East of Algeria). Rev. des Sci. la Technol. 25, 1–15.
Hilly, J., 1962. Étude géologique du Massif de l'Edough et du Cap de Fer (Est-Constantinois). These de la Faculté des Sciences, Université de Nancy, France.
Hiscock, K.M., 2009. Hydrogeology: principles and practice. Hoboken, NJ: John Wiley & Sons.
Hounslow, A.W., 1995. Water quality data: Analysis and interpretation. Boca Raton, FL: Lewis.
Joleaud, L., 1936. Étude géologique de la région de Bône et de la Calle. La typo-litho & Jules Carbonel. Alger.

Kaufman, S., Libby, W.F., 1954. The natural distribution of tritium. Phys. Rev. 93, 1337–1344.

Kendall, C., 1998. Tracing Nitrogen Sources and Cycling in Catchments. Isot. Tracers Catchment Hydrol. 519–576.

Kjerfve, B., 1994. Coastal lagoons, in: Kjerfve, B. (Ed.), Elsevier Oceanography Series, Coastal Lagoon Processes. pp. 1–8.

Kock, S.T., Schittek, K., Wissel, H., Vos, H., Ohlendorf, C., Schäbitz, F., Lupo, L.C., Kulemeyer, J.J., Lücke, A., 2019. Stable Oxygen Isotope Records (δ18O) of a High-Andean Cushion Peatland in NW Argentina (24° S) Imply South American Summer Monsoon Related Moisture Changes During the Late Holocene. Front. Earth Sci. 7, 1–18. https://doi.org/doi: 10.3389/feart.2019.00045

Lasagna, M., De Luca, D.A., 2017. Evaluation of sources and fate of nitrates in the western Po plain groundwater (Italy) using nitrogen and boron isotopes. Environ. Sci. Pollut. Res. 26, 2089–2104.

Leahy, P.P., Rosenshein, J.S., Knopman, D.S., 1990. Implementation plan for the national water-quality assessment program. USGS Open- File Report 90-174, Denver, USA.

Lee, R.W., 1985. Geochemistry of groundwater in Cretaceous sediments of the southeastern Coastal Plain of eastern Mississippi and western Alabama. Water Resour. Res. 21, 1545–1556.

Letouzey, J., Trémolières, P., 1980. Paleo-stress fields around the Mediterranean since the Mesozoic derived from microtectonics : comparisons with plate tectonic data data. B.R.G.M. theisis 115, 261–273.

Li, J., Zhu, D., Zhang, S., Yang, G., Zhao, Y., Zhou, C., Lin, Y., Zou, S., 2022. Application of the hydrochemistry, stable isotopes and MixSIAR model to identify nitrate sources and transformations in surface water and groundwater of an intensive agricultural karst wetland in Guilin, China. Ecotoxicol. Environ. Saf. 231, 1–11.

Llavsky, J., Snopkova, P., 1987. Découverte d'Acritarches Paleozoiques dans les terrains métamorphiques de l'Edough (wilaya d'Annaba, Algérie). Comptes Rendus l'Academie des Sci. 305, 881–884.

Lyra, A., Loukas, A., Sidiropoulos, P., Tziatzios, G., Mylopoulos, N., 2021. An integrated modeling system for the evaluation of water resources in coastal agricultural watersheds: application in Almyros Basin, Thessaly, Greece. Water 13, 1–33.

Malki, M., Bouchaou, L., Hirich, A., Ait Brahim, Y., Choukr-Allah, R., 2017. Impact of agricultural practices on groundwater quality in intensive irrigated area of Chtouka-Massa, Morocco. Sci. Total Environ. 574, 760–770.

McCance, W., Jones, O.A.H., Edwards, M., Surapaneni, A., Chadalavada, S., Currell, M., 2018. Contaminants of Emerging Concern as novel groundwater tracers for delineating wastewater impacts in urban and peri-urban areas. Water Res. 146, 118–133.

Mebrouk, N., Blavoux, B., Issadi, A., Marc, V., 2007. Geochemical and isotopic characterization of high-mg ground waters in Endorheic basin, Ain oussera Algeria. J. Environ. Hydrol. 15, 1–20.

Menció, A., Casamitjana, X., Mas-Pla, J., Coll, N., Compte, J., Martinoy, M., Pascual, J., Quintana, X.D., 2017. Groundwater dependence of coastal lagoons: the case of La Pletera salt marshes (NE Catalonia). J. Hydrol. 552, 793–806.

Mengis, M., Schiff, S.L., Harris, M., English, M.C., Aravena, R., Elgood, R.J., MacLean,

A., 1999. Multiple geochemical and isotopic approaches for assessing ground water NO3 - Elimination in a riparian zone. Ground Water 37, 448–457.

Moulla, A.S., Guendouz, A., 1996. A survey of rainwater chemical and isotopic composition in North Algeria, in: Séminaire International Sur l'Application Des Techniques Isotopiques Dans Le Domaine Des Ressources En Eau et En Sol. Mahdia, Tunisia. pp. 14–18.

Mourdi, W., 2011. Pollution urbaine, impact sur l'homme et l'environnement '"cas de l'agglomération de Annaba et ses environs."' Master's thesis, Université d'Annaba, Algérie.

Nadhir, A., 2019. Étude de la pollution atmosphérique en provenance de la zone pétrochimique de la ville de Skikda. Ph.D thesis, Université de Skikda, Algérie.

Newton, A., Brito, A.C., Icely, J.D., Derolez, V., Clara, I., Angus, S., Schernewski, G., Inácio, M., Lillebø, A.I., Sousa, A.I., Béjaoui, B., Solidoro, C., Tosic, M., Cañedo-Argüelles, M., Yamamuro, M., Reizopoulou, S., Tseng, H.C., Canu, D., Roselli, L., Maanan, M., Cristina, S., Ruiz-Fernández, A.C., De Lima, R.F., Kjerfve, B., Rubio-Cisneros, N., Pérez-Ruzafa, A., Marcos, C., Pastres, R., Pranovi, F., Snoussi, M., Turpie, J., Tuchkovenko, Y., Dyack, B., Brookes, J., Povilanskas, R., Khokhlov, V., 2018. Assessing, quantifying and valuing the ecosystem services of coastal lagoons. J. Nat. Conserv. 44, 50–65.

Panno, S.V., Kelly, W.R., Martinsek, A.T., Hackley, K.C., 2006. Estimating background and threshold nitrate concentrations using probability graphs. Ground Water 44, 697–709.

Park, J., Sanford, R.A., Bethke, C.M., 2009. Microbial activity and chemical weathering in the Middendorf aquifer, South Carolina. Chem. Geol. 258, 232–241.

Penna, D., Stenni, B., Šanda, M., Wrede, S., Bogaard, T.A., Gobbi, A., Borga, M., Fischer, B.M.C., Bonazza, M., Chárová, Z., 2010. On the reproducibility and repeatability of laser absorption spectroscopy measurements for δ 2 H and δ 18 O isotopic analysis. Hydrol. Earth Syst. Sci. 14, 1551–1566.

Pittalis, D., Carrey, R., Da Pelo, S., Carletti, A., Biddau, R., Cidu, R., Celico, F., Soler, A., Ghiglieri, G., 2018. Hydrogeological and multi-isotopic approach to define nitrate pollution and denitrification processes in a coastal aquifer (Sardinia, Italy). Hydrogeol. J. 26, 2021–2040.

Rachid, G., Alameddine, I., El-Fadel, M., 2021. SWOT risk analysis towards sustainable aquifer management along the Eastern Mediterranean. J. Environ. Manage. 279, 1–15.

Rao, N.S., Ghermandi, A., Portela, R., Wang, X., 2015. Global values of coastal ecosystem services: A spatial economic analysis of shoreline protection values. Ecosyst. Serv. 11, 95–105.

Samraoui, B., De Belair, G., 1997. The Guerbes-Sanhadja wetlands, Part I, Overview. Ecology 28, 233–250.

Sigman, D.M., Casciotti, K.L., Andreani, M., Barford, C., Galanter, M., Böhlke, J.K., 2001. A bacterial method for the nitrogen isotopic analysis of nitrate in seawater and freshwater. Anal. Chem. 73, 4145–4153.

Singleton, M.J., Esser, B.K., Moran, J.E., Hudson, G.B., Mcnab, W.W., Harter, T., 2007. Saturated zone denitrification: Potential for natural attenuation of nitrate contamination in shallow groundwater under dairy operations. Environ. Sci. Technol.

41, 759–765.
Stock, B.C., Jackson, A.L., Ward, E.J., Parnell, A.C., Phillips, D.L., Semmens, B.X., 2018. Analyzing mixing systems using a new generation of Bayesian tracer mixing models. PeerJ 6, e5096. https://doi.org/https://doi.org/10.7717/peerj.5096.
Stumpp, C., Ekdal, A., Gönenc, I.E., Maloszewski, P., 2014. Hydrological dynamics of water sources in a Mediterranean lagoon. Hydrol. Earth Syst. Sci. 18, 4825–4837.
Tantawi, M.A., El-Sayed, E., Awad, M.A., 1998. Hydrochemical and stable isotope study of groundwater in the Saint Catherine-Wadi Feiran area, South Sinai, Egypt. J. African Earth Sci. 26, 277–284.
Thatcher, L.L., Janzer, V.J., Edwards, K.W., 1977. Methods for Determination of Radioactive Substances in Water and Fluvial Sediments, Techniques of Water-resources. Investigations of the United States Geological Survey. U.S. Geological Survey, Washington, United States.
Toran, L.E., Saunders, J.A., 1999. Modeling alternative paths of chemical evolution of Na-HCO3-type groundwater near Oak Ridge, Tennessee, USA. Hydrogeol. J. 7, 355–364.
Torres-Martínez, J.A., Mora, A., Mahlknecht, J., Daessle, L.W., Cervantes-Aviles, P.A., Ledesma-Ruiz, R., 2021. Estimation of nitrate pollution sources and transformations in groundwater of an intensive livestock-agricultural area (Comarca Lagunera), combining major ions, stable isotopes and MixSIAR model. Environ. Pollut. 269, 1–12.
Toubal, O., Boussehaba, A., Toubal, A., Samraoui, B., 2014. Biodiversité méditerranéenne etchangements globaux : cas ducomplexe de zones humides deGuerbès-Senhadja (Algérie). Physio-Géo 8, 273–295.
Tremblay, R., Walter, J., Chesnaux, R., Boumaiza, L., 2021. Investigating the potential role of geological context on groundwater quality: a case study of the Grenville and St. Lawrence Platform geological provinces in Quebec, Canada. Geosci. 11, 1–21.
Velasco, A.M., Pérez-Ruzafa, A., Martínez-Paz, J.M., Marcos, C., 2018. Ecosystem services and main environmental risks in a coastal lagoon (Mar Menor, Murcia, SE Spain): the public perception. J. Nat. Conserv. 43, 180–189.
Vila, J.M., 1980. La chaîne alpine d'Algérie orientale et des confins Algéro-tunisiens. Ph.D thesis, Université de Pierre et Marie- Curie, France.
Vystavna, Y., Schmidt, S.I., Diadin, D., Rossi, P.M., Vergeles, Y., Erostate, M., Yermakovych, I., Yakovlev, V., Knëoller, K., Vadillo, I., 2019. Multi-tracing of recharge seasonality and contamination in groundwater: a tool for urban water resource management. Water Res. 161, 413–422.
Walter, J., Chesnaux, R., Cloutier, V., Gaboury, D., 2017. The influence of water/rock − water/clay interactions and mixing in the salinization processes of groundwater. J. Hydrol. Reg. Stud. 13, 168–188.
Wassenaar, L.I., 1995. Evaluation of the origin and fate of nitrate in the Abbotsford Aquifer using the isotopes of15N and18O in NO3-. Appl. Geochemistry 10, 391–405.
WHO, (World Health Organization), 2017. Guidelines for drinking-water quality, 4th edition, incorporating the 1st addendum. ISBN: 978-92-4-154995-0.
Willaert, T.O.M., 2014. Valuation of marine and coastal ecosystems: The role of ecological-economic modeling. Master's thesis, Universidade Nova de Lisboa, Portugal.
Zhang, Y., Li, F., Zhang, Q., Li, J., Liu, Q., 2014. . Tracing nitrate pollution sources and

transformations in surface- and ground-waters using environmental isotopes. Sci. Total Environ. 490, 213–222.